2012

Catalytic Oxidative Desulfurization: A Comparison of Reactors

Andrew Marshall Madrid
Louisiana State University and Agricultural and Mechanical College, amadri1@lsu.edu

CATALYTIC OXIDATIVE DESULFURIZATION: A COMPARISON OF REACTORS

A Thesis

Submitted to the Graduate Faculty of the
Louisiana State University and
Agricultural and Mechanical College
in partial fulfillment of the
requirements for the degree of
Master of Sciences in Chemical Engineering

in

The Cain Department of Chemical Engineering

by
Andrew Madrid
B.S., University of Florida, 2010
December 2012

ACKNOWLEDGMENTS

I am grateful to Dr. Kerry Dooley and Dr. Carl Knopf for their assistance and for all of the knowledge they have imparted to me. Their work ethics were continually a source of inspiration to me, and a shining example of the professional I aspire to be. I also want to thank Dr. Roy at CAMD for his assistance with XRD and Dr. Dodla from the LSU AgCenter for the ICP-AES work. Joe Bell, Paul Rodriguez and all of their staff in the Chemical Engineering Department Shop were instrumental in the repairs and troubleshooting throughout the entire process. I also want to extend my gratitude to my student workers, Brian Fontenot, Ragan Gautier and Claire Hayes. Also, I wish to express my deep thanks to NSF for supporting this work. I must also thank my father, Larry Madrid, who shaped a legacy of engineering curiosity for me to follow, while setting an example of innovation, industry and integrity. Additionally, my dearest wife Chelsea must be commended for her support, grace and patience as I completed my thesis.

TABLE OF CONTENTS

INDEX OF ABBREVIATED TERMS

BET Brauner-Emett-Teller method

DBT dibenzothiophene

DMDBT dimethyl dibenzothiophene

DRIFTS diffuse reflectance infrared Fourier transform spectroscopy

FTIR Fourier transform infrared

GC gas chromatography

GC/MS gas chromatography/mass spectrometry

HDS hydrodesulfurization

ICP inductively coupled plasma (atomic emission spectroscopy)

MDBT methyldibenzothiophene

OBR oscillatory baffled reactor

ODS oxidative desulfurization

PID proportional-integral-derivative controller

POMR pulsed oscillating monolith reactor

PTFE polytetraflouroethylene

STR stirred tank reactor

TBHP tert-butylhydroperoxide

TOF turnover frequency

ULSD ultra low sulfur diesel

XRD X-ray diffraction

INDEX OF CATALYSIS TERMS

Conversion 100 x (mols Y at t=0 – mols Y at $t=t_1$) / (mols Y at t=0)

Dispersion (total metal surface sites) / (total metal atoms)

Overall Conversion (mols reagent at t=0 – mols reagent Y at $t=t_1$) / (mols reagent at t=0)

Reagent All oxidizable components in the feed

Selectivity 100 x (mols S-heterocycles at t=0 – mols S-heterocycles at $t=t_1$) /

(mols alkylaromatics at t=0 – mols alkylaromatics at $t=t_1$)

ABSTRACT

A novel technology, a pulsed oscillating monolith reactor (POMR), was compared to a standard autoclave reactor for oxidative desulfurization (ODS) of a model diesel fuel. Two classes of catalysts, mesoporous Ti-MCM-41 and Pd on carbon, were used for ODS. The oxidants used were O_2 and peroxide. The model diesel compound was 75 wt% alkanes, 24 wt% alkylaromatic, 0.95 wt% sulfur heterocycles and 0.05% nitrogen heterocycles. ODS reactions were conducted from 343-423 K and pressures from 1.0-1.3 MPa O_2. The only component that was not oxidized was the alkane.

The POMR showed promise; there was up to a factor of 20 enhancement in turnover frequency for alkylaromatics, up to a factor of 9 for sulfur heterocycles and up to 20 for nitrogen heterocycles. However, the POMR was no more selective and in some cases less selective when compared to runs performed in an autoclave.

It was determined that the Ti-MCM-41 has a higher initial catalytic activity then supported Pd, but it deactivates more quickly due to the condensation of products on the surface and in the pores. It additionally had a higher selectivity than the carbon-supported Pd. The Ti-MCM-41 catalyst specifically did a better job of oxidizing dibenzothiophene, which is one of the most refractory sulfur compounds.

There was no significant improvement from the substitution of benzoyl peroxide for O_2 as oxidant. Neither the sulfur compound turnover frequencies nor the overall dibenzothiophene conversion were improved, when roughly equal amounts of oxidant were provided.

CHAPTER 1 INTRODUCTION AND LITERATURE REVIEW

1.1 Legislation Driving the Change to Ultra Low Sulfur Diesel

Legislation following concerns about air quality and acid rain, caused partially by sulfur emissions, have spurred a wave of change in the fuels industry through most of the developed world. Beginning December 1, 2010, all highway diesel fuel available in the United States has been Ultra Low Sulfur Diesel (ULSD). ULSD sets a 15 ppm cap on the sulfur in diesel fuels.[3] The Environmental Protection Agency is responsible for these regulations (2001) that slowly phased out sulfur. Non-road diesel fuel was regulated at 500 ppm sulfur in 2007 and to 15 ppm in 2010. Railroad locomotive and marine diesel fuels were also decreased to 500 ppm sulfur in 2007, and in 2012 changed to ULSD. There are exemptions for small refiners of non-road, locomotive and marine diesel fuel that allow for 500 ppm diesel to remain in the system until 2014. December 1, 2014 is the date that USLD for all highway, non-road, locomotive and marine diesel fuel in the United States will be mandatory.

European regulations stemming from EU Directive 2005/33/EC legislate sulfur reductions in highway diesel down to 10 ppm by 2009, which further tightened regulations from 50 ppm as mandated by Directive 1999/32/EC. Japan imposed a decrease from 500 to 50 ppm by the end of 2004 and is planning to further lower this limit to 10 ppm by 2007.[4]

1.2 The Need for Oxidative Desulfurization

Obtaining ULSD by current hydrodesulfurization (HDS) technology requires a high reaction temperature, high reaction pressure greatly expanding capital costs, expensive H_2 gas, and a large reactor volume. HDS experiences difficulties in converting alkyl substituted heterocyclic sulfur-containing compounds, for example 4-methyldibenzothiophene and 4,6-dimethyldibenzothiophene (4,6-DMDBT), shown in Fig. 1.1.[5] The hydrogenation is drastically

affected by steric constraints, and is further complicated by the C-S bond having similar bond energy to the C-H bond.[5b] The current process of HDS can use up to 60% of the hydrogen needed to remove 99% of the sulfur and then use the remaining 40% to remove that remaining 1%.[6] The large spike in H_2 consumption toward the end of the process is not only expensive, but undesirably ends up hydrogenating other aromatic components of the feed.

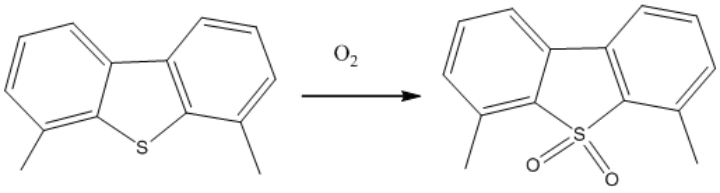

Figure 1.1 Oxidation of 4,6-DMDBT to sulfone

ODS can be conducted at relatively mild conditions compared to HDS, usually 313-373 K and 0.1-0.2 MPa total pressure.[7] The sulfur compounds are oxidized into the corresponding sulfoxides / sulfones (Fig. 1.1), which are polar and can be removed by polar solvents (acetonitrile, methanol, *N*,*N*-dimethylformamide, etc.) or adsorbed out of solution on activated carbon.[7-8] Contrary to HDS, the refractory aromatic sulfur-containing molecules such as the derivatives of DBT can be more easily converted to their sulfones than is thiophene, and thiols.[7, 9] Electron donation of alkyl groups to the ring structure favors the attachment of the heterocycle at the sulfur adsorbing site. Oxidants include H_2O_2, surface-bound –OOH, organic peroxides, aldehydes with O_2, and possibly O_2 itself.[7-8, 10]

1.3 ODS with Oxygen

There are few publications in this category relative to the other methods. Sampanthar et al. reported that $MnO_2/\gamma\text{-}Al_2O_3$ and $Co_3O_4/\gamma\text{-}Al_2O_3$ can catalyze the air oxidation of the refractory sulfur impurities in real diesel to their corresponding sulfones at 403-473 K and 0.1 MPa air.[11] The sulfur content was reduced to 40-60 from 400 ppm in the feed after extraction by

1-methyl-2-pyrrolidinone (NMP). The cost of this oxidation was high, however, with the olefin content of the diesel increasing from 2.4 % to 3.6 %, and the aromatic content decreasing from 46.4% to 12.5%, while the cetane index increased by 20%. All of these changes are indicative of the oxidation of aromatics in the treated diesel. There was also evidence of SO_2 in the scrubbed outlet gas. Oxidation was not possible below 383 K, even with a high Mn loading on Al_2O_3. However, for Co_3O_4/Al_2O_3, differences in Co-loading did not lead to significant differences in conversion. The sulfur reactivity of this system was: 4, 6-DEDBT > 4, 6-DMDBT > 4-MDBT > DBT. The highest turnover frequency (TOF) for S oxidation, 7.8×10^{-3} s^{-1}, was reported at 423 K. The catalyst activity for different sulfur-containing compounds at 573 K (95% conversion) was: thiophene, at O/S molar ratio = 110 and WHSV = 7 h^{-1}; DBT, at O/S = 95 and WHSV = 13 h^{-1}; 1-pentanethiol and dibutyl sulfide, O/S = 10~15 and WHSV = 30 h^{-1}. It was found via infrared spectroscopy (DRIFTS) that the adsorption of thiophene took place at room temperature, and was easier than the adsorption of paraffinic, olefinic, and aromatic hydrocarbons. But the main finding was that by raising the temperature of the oxidation above 373 K there was significant oxidation of the aromatic components of the diesel feed.

Further findings by Song et al. showed that a model jet fuel with 747 ppm of S can be oxidized with O_2 using Fe(III) salts, the nitrate and the bromide, with a wt. ratio of 1/3 supported on activated carbon, at 25°C and 0.1 MPa. [7] The relative order of sulfur heterocycle reactivity was 2-methylbenzothiophene > 5-methylbenzothiophene > benzothiophene >> dibenzothiophene. The catalyst converted 38% of the DBTs and BTs to sulfones in 5 h with fuel/catalyst ratio of 21. The adsorption of S compounds on the activated carbon was also studied; the carbon had a higher adsorption selectivity for DBTs and sulfones than for BTs. This indicates that it might be a lot easier to find the sulfones on the catalyst surface than in solution,

especially in the case of low conversions or small reactor batches. It was also found that for an increased loading (33%) of Fe(III) salt, the oxidation activity increased, proving that Fe was involved in forming the active site.

1.4 ODS with Oxygen and Aldehyde

Most previous ODS research has centered around peroxide oxidants, and although peroxide ODS is attractive because the reaction conditions are mild, for plant scale operation the use and storage of peroxides is dangerous and expensive. This makes the generation of peroxide species in-situ an attractive alternative. Aldehydes can be used as sacrificial oxidants in ODS systems, because aldehydes can be oxidized under mild conditions with O_2 to peracids, which in turn oxidize the sulfur compounds.[8, 10c] Murata proposed the following.[8]

$$C_7H_{15}CHO + O_2 \rightarrow C_7H_{15}CO_3H \qquad (1)$$

$$DBT + 2\ C_7H_{15}CO_3H \dashrightarrow DBT\ sulfone + 2\ C_7H_{15}CO_2H \qquad (2)$$

This method, using a cobalt catalyst in atmospheric oxygen, achieved 97% sulfur removal. Murata proposed a chain-radical mechanism, where the aldehyde is oxidized by the metal salt to give a proton and an acyl radical (equation 3). The acyl radical incorporates O_2 easily, forming the acylperoxy radical (equation 4), which reacts with an aldehyde yielding a peracid and a regenerated acyl radical (equation 5). Two molecules of peroxyacid then oxidize the sulfur atom to form a sulfone (equations 6 and 7).

$$RCHO + M^{(n+1)+} \rightarrow RCO^* + H^+ + M^{n+} \qquad (3)$$

$$RCO^* + O_2 \rightarrow RCO_3^* \qquad (4)$$

$$RCO^* + RCHO \rightarrow RCO_3H + RCO^* \qquad (5)$$

$$RCO_3H + R'SR' \rightarrow RCO_2H + R'SOR' \qquad (6)$$

$$RCO_3H + R'SOR' \rightarrow RCO_2H + R'SO_2R' \qquad (7)$$

1.5 ODS with Added Peroxide

Most ODS research has gone the added peroxide (e.g., H_2O_2, t-butylhydroperoxide,) route, with the products either sulfones or mixtures of sulfones and sulfoxides.[12] Hydrogen peroxide oxidation is a very attractive pathway from an environmental point of view, because its only theoretical byproduct is water.[13] The primary difficulty with aqueous H_2O_2 is its insolubility in hydrocarbons; the reacting system must be two phase.[14] This difficulty is lessened by using phase transfer agents. In Zhao et al. a formic acid/H_2O_2 system is used with quaternary ammonium salts and ultrasound, achieving a removal of 95% of the heterocyclic sulfur.[14] Otsuki used H_2O_2 and formic acid at 323 K under magnetic stirring, but was unable to achieve ODS of thiophene, 2-methylthiophene, and 2,5-dimethylthiophene.[10e] Oxidation was achieved for seven other sulfur species each and DFT calculations revealed a calculated a valence electron density of above 5.739 on the sulfur atom, with observed reactivity increasing with calculated electron density at the S atom. Reactivity of the species was found to be methyl phenyl sulfide > thiophenol > diphenyl sulfide > 4,6-DMDBT > 4-MDBT > DBT > 1-benzothiophene. The relative reactivities of the sulfur species were not linked to the composition of the organic solvent, which suggests that the solvent can affect the overall rate but not the mechanism.[10b] It was shown that the reaction rates increased when the C/H ratio of the solvent increased. The oxidation rate for the benzo- and dibenzothiophene could be approximated by pseudo-first order kinetics, but this was not the case for thiophenol, diphenyl sulfide, and butanethiol. Additionally, as no sulfoxide products were found, Otsuki et al. concluded that the rate determining step must be oxidation of the sulfide to sulfoxide.[10e]

Li et al. used a $[(C_{18}H_{37})_2N^+(CH_3)_2]_3$-$[PW_{12}O_{40}]$ catalyst with H_2O_2 to achieve a 500 to 0.1 ppm decrease of 4,6-DMDBT in diesel, with 100% selectivity to sulfones at temperatures

ranging from 303 to 363 K, and reaction times for full conversion from 80 to 8 min.[15] The catalyst was chosen to give activity similar to quaternary ammonium salts, but to form a less stable emulsion, so it was easier to separate via centrifugation and recycle. There was 96% oxidant efficiency 100 x (mol oxidized 2,4-DMDBT)/(mol H_2O_2), and a turnover number higher than 300 for this catalyst.

Using t-butyl hydroperoxide as an oxidant has certain advantages. It is soluble in oil and so there is no need for an emulsion. Therefore it is not limited to batch reactors. Corma et al. discovered that in operating a fixed bed reactor with TBHP as an oxidant that not only was Ti-MCM-41 mesoporous titanosilicate more active than $MoOx/Al_2O_3$, but that there was no leaching of the Ti from the fixed bed. [16] It was also noted that when the polarity of the Ti silicalite was decreased by silylation the amount of sulfone adsorbed by the catalyst significantly decreased, allowing longer catalyst lifetimes. There is other work suggesting that mesoporous materials (e.g., Ti-HMS titanosilicate) can outperform comparable microporous materials (e.g., TS-1 titanosilicate). In turn this suggests that there must be large concentration gradients for S-heterocycles in conventional micropore catalysts.[12a, b]

Two Al_2O_3 supported heteropolyacids ($H_3PMo_{10}V_2O_{40}$ and $H_3PMo_{12}O_{40}$) were also compared for ODS application with pre-hydrotreated diesel using TBHP.[17] The $H_3PMo_{10}V_2O_{40}$ was more active, but the $H_3PMo_{12}O_{40}$ was more selective and had a lower TBHP consumption per turnover.

1.6 Oscillating Reactors

1.6.1 Ultrasound

Ultrasonic oscillations have become an increasingly popular method to increase the efficacy of ODS reactions. Ultrasound can be effectively used to increase the quality (interfacial

area) of the emulsion that often forms the reacting system, which can increase the observed reaction rate substantially. Mei et al. used a 0.5" titanium tipped ultrasonic probe suspended in 50 mL of diesel feed.[18] This system was capable of creating a very fine emulsion with high intensity ultrasound. The fuel was treated in the reactor with tetraoctyclammonium bromide, H_2O_2 and phosphotungstic acid at 348 K, 0.1 MPa, and 20 kHz, and the sulfone was then extracted with acetonitrile. In a model system of 0.4 wt% DBT dissolved in toluene, and in which ultrasound was used, within 1 min 85% of the DBT was oxidized, and within 3 min the conversion was up to 95%, with complete oxidation within 7 min. Conversely when there was no ultrasound there was only 21% oxidation in 1 min and only 80% conversion in 7 min. When using an actual diesel feed the time needed to lower the sulfur content without sonication by 98% was 4 h, but by adding an in-situ adsorption on silica to remove the sulfone this time was lessened to 10-18 min. Additionally, 4,6-DMDBT, the most refractory compound in traditional HDS, was completely converted to its sulfone in this process.

Mikkola used ultrasonic irradiation in an attempt to improve the activity of a recirculated Raney nickel catalyst for the hydrogenation of xylose to xylitol, and found that it improved selectivity and also decreased catalyst deactivation.[19] The apparatus consisted of a 0-100 W, 20 kHz generator, a piezoelectric transducer and a titanium horn, giving a 12 μm peak to peak amplitude when connected to the bottom of an autoclave. The energy supplied ranged from 0.2 to 0.4 W/mL. The deactivation rate constant at 373K and 4 MPa, was 6×10^{-3} min^{-1} with no oscillation and dropped to 4.5×10^{-3} min^{-1} with the ultrasound.

The sonochemistry resulting from cavitation creates localized high temperature and pressure regions. The energy at these acoustic cavitation hot spots is so high that there is even light emitted as the bubbles collapse.[20] The ultrasound creates, grows and collapses the bubbles

in fractions of a second. The reactive zone around the bubble extends only about 200 nm around the surface and has a lifetime of about 2 μs after collapse. The light emissions from the cavitations were studied in silicone oil at 277 K by examining the excited state C_2 emission spectra, and it was estimated that the temperature of the cavitation was 5075±156 K. [20a] The pressure calculated inside a cavitation bubble with concentrated sulfuric acid in 0.1 MPa Ar is 150 MPa.[21] The localized energy is so intense that irradiated 10 μm Zn particles suspended in solution underwent collisions at half the speed of sound and temperatures between 2900 and 3700 K and actually fused together.[20b, 22] In aqueous chemistry ultrasound leads to the formation of reactive species OH•, H•, and H_2O_2, and additionally Cl• and Cl_2 when chlorocarbons are irradiated.[23]

In heterogeneous catalysis, Suslick discovered that ultrasound enhances the hydrogenation activity of Ni powder by more than 10^5 times.[24] There was a marked change in the catalyst properties, with observable differences in the particle aggregation, surface morphology and surface oxide thickness for the particles. Nickel has essentially no activity for the hydrogenation of alkenes at 273 K and 1 atm H_2, with rates for 1-nonene hydrogenation less than 10 nM/min, whereas the irradiated sample has rates up to 1.5 mM/min. While the latter rate is comparable to that of specially made Raney Ni catalysts, the irradiated powder was shown to be more selective, leaving C-O bonds untouched. The cavitation slowly eroded the surface, reducing the oxidation layer on the catalyst from 25 nm to 5 nm in ~1 h. The slow erosion of the particles' surface does not appreciably change the suface area of the catalyst.[24]

There are startup companies currently working on commercializing an ultrasound ODS process, Sulphco has several patents for ODS using an ultrasonic probe technology.[25] Sulphco claims that the ultrasonic probe assists catalytic ODS with bubble cavitation, using high

frequency (18-20 kHz) and low amplitude (30-100 μm) oscillations. Sulphco claims to have developed a process that can effect ODS by ultrasound using H_2O_2 and titanium isopropoxide at 323-373 K.[25b] The process is continuous.

1.6.2 Pulsed Trickle Beds

Pulsed trickle beds work on the principle of pulsing the gas upward or downward through a packed bed and dripping feed downward. This provides a wetted area with low diffusional lengths for the gas to the catalyst surface, especially for the part of the cycle where the gas is pulsed "on". Trickle beds can operate reliably over a relatively large range of gas-to-liquid (G/L) ratios, but they have difficulties maintaining a uniform radial liquid distribution across the packing. It is common to experience channeling, which decreases the overall wetting efficiency. This is commonly the case for downflow trickle beds that operate with low liquid superficial velocities.[26] While sometimes the thin liquid films created by channeling can have a positive effect on observed rate,[27] it is more likely that channeling leads to hot spots, catalyst deactivation, and poor selectivity; therefore it is important to minimize channeling. A proven way to improve the feed distribution and so reduce channeling is to pulse the gas flow and possibly also the liquid flow, using a solenoid valve.[28] The pulsed flow rates can also increase the surface wetting (coverage of liquid on the catalyst during the liquid-rich part of the cycle) and also the removal of products from the surface (during the gas-rich part of the cycle), and can provide a more even radial temperature profile in the reactor. Increases in activity (observed rate) by as much as 60% and 10% were recorded for α-methyl-styrene hydrogenation in a pulsed trickle bed packed with a Pd/Al_2O_3 catalyst.[28a, 28f]

Additionally, gains in selectivity have been noted using the pulsed method. Wilhite et al. achieved a 45% increase in styrene selectivity during phenylacetylene hydrogenation by pulsing

the liquid feed; it was assumed that the periodic large nature of the liquid pulses more effectively removed the product from the catalyst surface, before it was fully hydrogenated, thereby increasing selectivity to styrene.[29]

It is difficult to pulse the liquid in a trickle bed reactor quickly, necessitating several minutes between pulses under many conditions. This is because there is a tendency for rapid pulses to recombine quickly and thereby negate the effects of pulsation. Conversely, Boelhouwer et al. were able to show that by increasing the superficial gas velocities and keeping the pulse times short, stable gas pulse behavior at up to 1 Hz could be attained, with minimal decay of pulses. Additionally, it was discovered that the liquid holdup and liquid velocity are only dependent on the superficial gas velocity.[28c]

1.6.3 Oscillatory Baffled Reactor

An oscillatory baffled reactor (OBR) is a novel continuous reactor structured similarly to a stirred tank reactor (STR), but instead of the motor shaft and attached impeller turning radially, the shaft is instead attached to an insert with equally spaced orifice baffles, and oscillated up and down in the cylindrical tank.[30] It can provide efficient compartmental mixing while still maintaining near-plug flow. The reactor allows for a greater control of mixing as both the shape of the baffles and the speed of oscillation can be changed.[31] Wilson et al. investigated the improvement of the OBR over an STR for the phase-transfer catalyzed reaction of n-butyl bromide and sodium phenolate using both tetra-n-butyl ammonium bromide and benzyltributyl ammonium bromide quaternary ammonium salts. Another advantage to this reactor is its compatibility with heterogeneous catalysts. It was able to suspend 250 μm diameter glass pellets coated with TiO_2 even at mild power dissipation levels.[32] This reactor was used by Watson for the transesterification of rapeseed oil to ‘biodiesel’ and was found to be produce a suitable

product (cetane number = 45) in substantially lower time than batch processes, having a residence time of 30 min at 323 K.

1.7 The Goal of This Research Work

It is hypothesized that any practical ODS process must rely on in-situ peroxide or peracid production using catalysts tailored for this purpose. The goal of this work is to investigate the performance of desulfurization catalysts with O_2 as the initial oxidant to oxidize sulfur heterocycles, while minimizing the oxidation of the non-sulfur compounds in the system. The most easily oxidized non-sulfur compounds are the alkyaromatics, cycloalkanes and indans. Another goal was to identify as many of the oxidation products as possible. Finally, it was desired to know the fate of the N-containing heterocycles in the oxidations, and how much they affected the oxidation of the S-containing heterocycles.

CHAPTER 2 EXPERIMENTAL METHODS

2.1 Feed Composition

The feed used was modeled after a No 2 Diesel and was made with 75 wt% n-hexadecane (ChemSampCo, 95-96%), 12% ethylbenzene (Sigma Aldrich, 99%), 12% 2-methylnaphthalene (Acros Organics, 95-97%), 0.55% dibenzothiophene (Aldrich, 98%), 0.4% thiophene (Aldrich, 99+%), 0.03% carbazole (Aldrich, 99%), 0.02% acridine (Kodak).[33] For certain experiments the lighter compounds were excluded, and in this case the feed composition was 75% n-hexadecane 24% 2-methylnaphthalene, 0.95% dibenzothiophene, 0.03% carbazole, 0.02% acridine.

2.2 Semibatch Rocking Reactor

The rocking reactor is a heating block which contains 4 slots for separate 20 mL 316 stainless steel reactors shown in Fig. 2.1. Each has a manual control valve on top and the four are fed through a single line attached to an O_2 cylinder (Capital Welders, 99.9%). The catalysts used were reduced outside of the system, and quickly added and submerged in the feed. A K-thermocouple mounted into the center of the heating block supplied the measured input to a PID temperature controller (Eurotherm 2116), and the temperature fluctuations were around 1 K. The runs were conducted with either of the model diesel feeds, the one made without the lights and the standard one. Each run was conducted with 0.1 g of catalyst at 1.13 MPa. The system was pressurized and purged several times prior to heating to obtain a pure O_2 atmosphere inside the vessels, then the valves were closed. The time was started once the samples came to temperature, the rocking initiated, and the valves opened and the vessels were brought back up to pressure. When the run was over the valves were closed and the reactors were removed from the block to speed the cooling. Then the samples were removed only after the reactors were

completely cool, and the samples were syringe filtered to remove the loose catalyst powder. They were then bottled and placed in a refrigerator for later analysis.

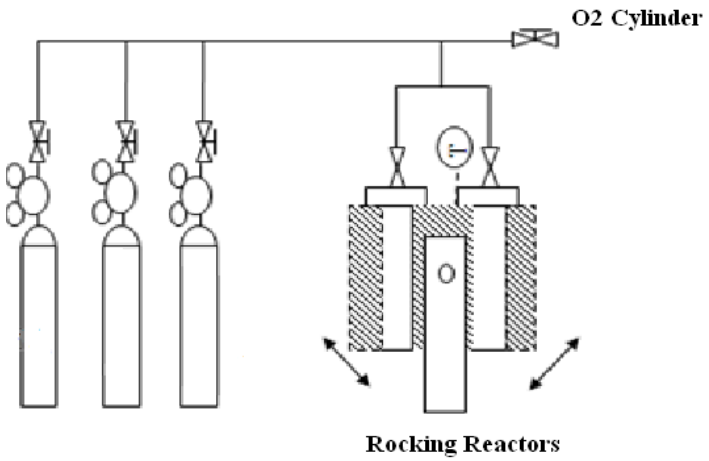

Figure 2.1 Rocking reactor, as modified from Liu [1]

2.3 Autoclave Reactor

A 500 mL Autoclave stirred reactor was configured with a K-thermocouple, a sampling valve and a feed line from the O_2 cylinder. The reactor was pressurized and purged several times before it was heated. The reactor was heated by a heating tape controlled by a PID controller (Eurotherm 2116). This setup yielded a +/-2 K temperature variation around the set point. The catalyst was loaded into a basket on the rotating shaft of the autoclave. The autoclave operated at its maximum speed, greater than 100 rpm. These reactions used the same feed to catalyst ratio as the rocking reactor runs, with 225 mL of feed and 2.25 g of catalyst. The experiments typically were for 96 h at 363 K and 1.13 MPa with a 30 minute period for heating up.

2.4 Pulsed Oscillating Monolith Reactor Runs

The pulsed oscillating monolith reactor (POMR) configuration is shown in Fig. 2.2. It is a square stainless steel reactor loaded with 10.8 x 10.8 x 8.2 cm depth monoliths and custom micro-channel heat exchangers, with holes through the heat exchangers lining up with the monoliths; the heat exchanger - reactor setup is shown in Fig. 2.3. The entire assembly is

sandwiched together above a PTFE diaphragm with a diameter of 17.8 cm. The POMR is placed inside a Yamato DKN 400 convection oven which, along with the heat exchangers through which Valvoline Dextron Transmission Fluid was pumped from a heating bath, kept the system at +/- 1°C. This diaphragm is attached to a piston housed in a lower compartment that was also pressurized to equalize the pressure on both sides of the diaphragm; this was to keep the diaphragm from bursting. The piston is then driven by a motor to propagate small pressure waves through the reactor. The amplitude of the piston was set to 2.5 mm, this distance being constrained by the mechanical stress a larger amplitude would place on the PTFE diaphragm. The maximum frequency used here was 15 Hz. Between the diaphragm and the first monolith was an air distributor through which the air was recirculated up through the monoliths and then through the rest of the system by a Maximator DLE5-1 gas booster pump.

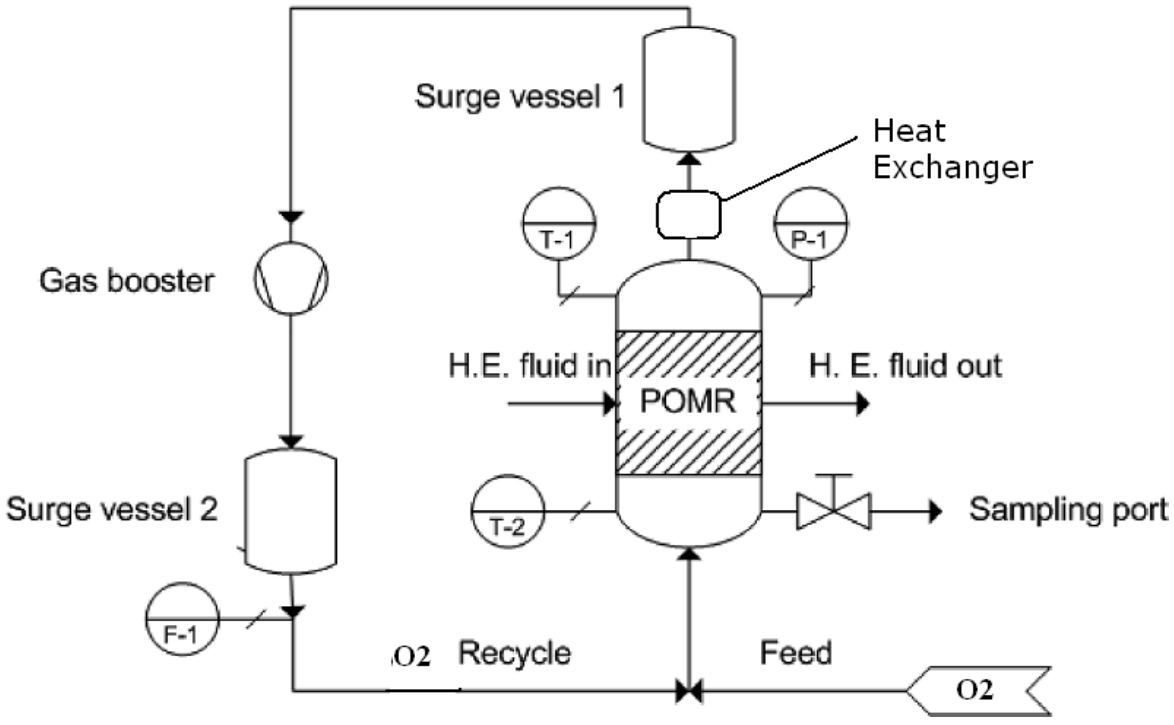

Figure 2.2 POMR configuration[2]

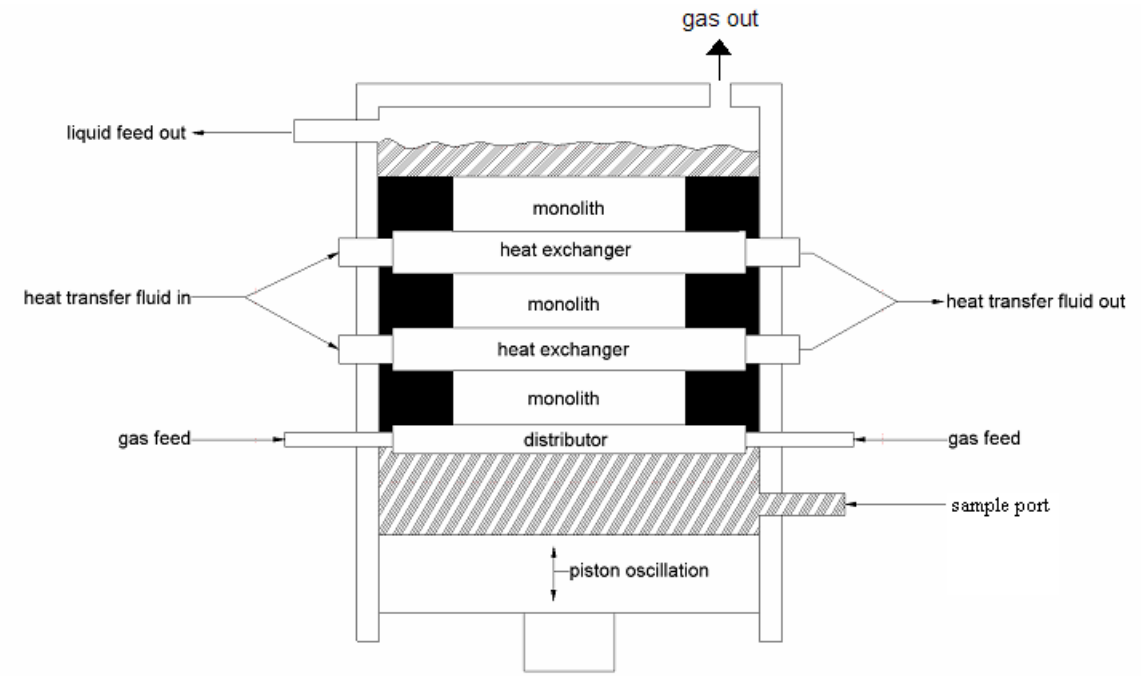

Figure 2.3 POMR cross-section[2]

The reactor was loaded with catalyst, pressure tested up to 1.13 MPa, purged, and then the catalyst reduced in 20% H_2/80% N_2 at 90°C overnight, at 0.11 MPa, with a slow release of gas out of the system through a bubbler. The reactor was then cooled to room temperature, and the valve to the bubbler was fully opened so the displaced gas could escape when a charge of 750 mL+/- 10 mL of feed was then loaded into the reactor. The reactor was then purged of the remaining H_2/N_2 gas, filled to atmospheric pressure with O_2 and left at 323 K overnight. It took about 1.5 hours of heating at 373 K to reach the 363 K desired temperature. Only after the reaction temperature was reached was the O_2 gas pressurized to 1.13 MPa in the system, the recirculation pump activated and the oscillations started. During the run the samples were taken from the sample port. The liquid feed is meant to be retained in the POMR compartment. There is a surge tank on both the bottom and top of the reactor to mitigate the large pressure swings caused by the recirculation pump.

2.5 Runs with Benzoyl Peroxide

Runs with additional benzoyl peroxide oxidant were carried out in both the autoclave reactor and the POMR. Enough peroxide was used in a run to convert approximately 20 mole percent of the oxidizable products, which does not include hexadecane.

2.6 Catalysts

Several types of catalysts were used for the experiments, both commercial and synthesized. The commercial catalysts were Sud-Chemie MPT-5 5% Pd/carbon powder, BASF/Engelhard 5% Pd/carbon powder, Lot # SE10217 (called Pd/E here), Degussa E5 5% Pd/carbon powder, Lot # B8692094, and cobalt octoate (Nuodex, 6% Co with octoate ligands in methanol).

The catalysts that were synthesized included Pd/carbons and mesoporous titanium silicates. The carbons were affixed to cordierite monoliths by a dipping process. The monoliths (200 cpsi, 5 × 5 × 1.2 cm, 1.3 mm hole diameter) were first boiled in deionized water for 3 h to clean impurities from the surfaces. A standard activated carbon (Calgon PCB 6X16) was washed with 1 M HNO_3 overnight with gentle stirring. The acid-treated carbon was washed with deionized water until the pH of the washings was > 4, and then dried in an oven at 100°C overnight. The carbon was then ground in a porcelain mortar and pestle and sieved to recover particles passing >200 mesh. These particles were then bound to the monolith using a polymerizing resin. The polymerization method (here called CMN-3) used a resorcinol-formaldehyde-copolymer gel whose setting behavior is based on controlling the amount of acid catalyst.[1] The gel was formed by dissolving 4.9 g resorcinol (Acros Organics, 98%) and 4.9 g Pluroinc F-127 copolymer (BASF) in 20 mL ethanol, adding 20 mL 3M HCL while stirring, and then 5.3 mL 37% aqueous formaldehyde solution (Acros) drop by drop. The suspension was

stirred until it began to thicken, the ideal time range for this being 20-30 min. Any faster reaction time made it very difficult to coat the monoliths before the resin set. The solution first became turbid and eventually started to separate into two zones. The top layer was decanted and discarded. The ground and sieved Calgon PCB carbon was added immediately prior to coating the mixture onto the monolith at a 0.25 to 1 Calgon/gel ratio. The most effective way to coat the monolith was to pour the gel onto the top of the monolith until it was evenly covered, and then to blow compressed air through a needle to clear the holes of gel. Then the monolith was turned over and this process repeated. In the event that some of the monolith channels were not cleared a paperclip worked well to push the gel through.

The coated monoliths were then dried at 353 K for 24 h and at 393 K for 24 h. Other coats were added as necessary to reach near 5% carbon loading on the monoliths. Then the monoliths were calcined in a Lindberg 55347 3-zone tube furnace with a 3'x3" quartz tube at a N_2 flow of 350 mL/ min, while the temperature was ramped from 393 to 673 K at 1 K/min with a 3 h hold, then from 673 to 1123 K at 5 K/min with a 3 h hold, then cooled at 5 K/min to 673 K prior to removal.

After the monolith was calcined and weighed the Pd was deposited on the support by a deposition-precipitation method as follows. The precursor solution was $PdCl_2$ dissolved in about 200 mL of 0.1 M HCl/g. A 20% excess of this solution (on a Pd basis) was deposited onto the dry carbon with a goal of 5% Pd loading on the carbon. The monoliths were suspended in the solution which was slowly stirring, while 0.1 M NaOH was added drop-wise to bring the pH to 12. After stirring for another 1 h, the monoliths were washed with water several times until the pH of the washings was below 9. The wash solutions were saved for ICP analysis. The monoliths were then dried in an oven at ~373 K for a few h or overnight, and then sealed until

they were reduced immediately prior to use. The reduction was accomplished at 523 K, with a 5 K/min ramp from 373 K, in a 10% H_2/90% N_2. The Pd deposition method was adapted from Dantas-Ramos et al.[34] and Toebes et al[35]

One powder catalyst that was used was synthesized by Liu using a mesoporous carbon support; it is called CDX-7(2).[1] It had a Pd loading of 3.9% and a H_2 dispersion of 78%. Two other carbon catalysts were also made, called PdP-01 and OMC5-1F. PdP-1 started with 5 g of Calgon PCB carbon of mesh 100-200. This size would be retained by screens made to hold it in place inside the POMR (the screens were 200 mesh). This carbon had the Pd precipitated on it using the same procedure as above. It was then vacuum filtered until the pH of the washings was below 9. The sample was then dried, calcined at 523 K for 3 h in a quartz cell in flowing H_2/N_2, and then cooled and bottled. OMC-5-1F was prepared identically except it was made from a mesoporous carbon prepared by Liu using his mesoporous carbon method 1, but with an oligomeric sucrose polyol solution (Rubicon) substituted for sucrose.[1]

The two mesoporous titanium silicates (Ti-MCM-41 structures) that were synthesized were made using the exact same procedure but with different starting components. A "Corma"-type synthesis used molar ratios of 1 SiO_2 (hydrophobic fumed silica):0.015 $Ti(OEt)_4$ (Sigma-Aldrich, 97%):0.26 cetyltrimethylammonium bromide (Aldrich):0.26 tetramethylammonium hydroxide (Acros Organics, 25 wt% in methanol):24.3 H_2O.[16] An "Eimer"-type synthesis used molar ratios of 1 Si (tetraethylorthosilicate, Aldrich, 98%): 0.0167 $Ti(OEt)_4$: 0.3 TMAOH : 0.4 CTABr : 60 H_2O.[36]

In both methods a 500 mL PTFE reactor with stir bar was used, immersed in a water bath atop a heater-stirrer. The excess water, silicon source and titanium source were mixed vigorously for 30 min, and the surfactant and template solutions were then added from two

separate burettes over a period of 1 h. The mixture was stirred at room temperature another 3 h. The system was then purged with N_2, heated to 363 K with the top on loosely to allow some gas to escape, and held for 1 h. Then the top was fully tightened, the temperature raised to 373 K, and the mixture reacted for three days. The precipitate was then filtered and washed with deionoized water, until neutral pH, then dried under vacuum for one day at 333 K. The powder was calcined in the 3-zone furnace in flowing N_2, ramped at 2 K/minute to 773 K, held 6 h or longer, then switched to air for another 6 h. Then the powder was cooled and bottled.

The Ti-MCM-41 was coated onto alumina pellets(Englehard 3945E 1/12") from a slurry consisting of 1 part Ti-MCM-41, 5 parts isobutanol and one part ethanol by weight. This was used to make 35 g of the slurry and stirred covered overnight. Then 3.249 g of dry alumina pellets were added to the slurry and allowed to soak overnight. The pellets were removed and dried slowly, ramping the temperature to 423 K and then holding overnight.

A different method was used to coat the cordierite monoliths, using a mixture of 50 wt % SASOL Dispal alumina and 50 wt % "Eimer" Ti-MCM-41. This method was adapted from a method used to coat alumina on cordierite by Bussard.[2] The monoliths were washcoated from a stirred aqueous slurry, at 25 wt % solids content, with 0.1 mol/L nitric acid added dropwise to maintain the pH at 3.5-4. Dry, bare monoliths that had been boiled in deionized water were dipped into the slurry, and excess slurry was removed with compressed air and a needle attachment. The coated monoliths were dried at 363 K, calcined at 773 K, reduced at 403 K in 10% H_2/N_2, and then bottled.

2.7 Product Analysis

2.7.1 FTIR

Fourier Transform Infrared (FTIR) spectroscopy of product samples and catalyst extracts was performed on a Mattson Infinity Gold FTIR. The solvents used to extract products from the catalysts were dichloromethane, acetone and a mixture of 50/50 ethanol and water. The extractions were carried out in a water cooled distillation column, where the solvent was left to boil for >8 h. The samples were loaded between KBr salt plates. The instrument settings were 64 scans of the sample and 32 of the background, a resolution of 4 and gain of 1.

2.7.2 Gas Chromatography

Routine Gas Chromatography (GC) analysis was conducted using a HP-5890 with an flame ionization detector (FID), and an Alltech EC-1 column with dimensions 30m x 0.32mm x 0.25µm. The temperature program was 333 K for 1 min, then ramped at 3.0 K/min until 342 K, then 5.0 K/min until 438 K, 15 K/min until 483 K, and a final hold of 19 min. The injector and detector were set to 523 K. The column flow was set to 1.8 min retention time for heptane with no purge. All samples were shot in at least triplicate. Mesitylene (Acros, 97%) was used as internal standard, at 1 vol. % of the solution (later switched to 3%). The retention time for the DBT sulfone product was determined using dibenzothiophene sulfone (Aldrich, 97%) dissolved in feed AM-Fd-5. The calibration can be found in Appendix A and was taken from Liu.[1]

2.7.3 GC/MS

GC/MS of selected product samples was conducted with a HP5890 Series II paired with a HP 5972 series Mass Selective (EI) Detector. The column initially used was a Supelco SP-2380, 30 m x 0.25mm x 0.25 µm, and later a 30 m x 0.32 mm x 0.25 µm Phenomenex ZB-1. The injection volume was varied between 0.2 and 2 µL in order to gain an appreciable signal. The

column flow was set to a methanol retention time of 1.3-1.4 minutes, with a 35 mL/min split. The 1992 version of the NBS75k database was used to identify the components of the sample. The inlet of the GC was set at 503 K, while the inlet to the MS was at 473 K. The temperature program was from 413 K with a ramp rate of 10 K/min until 498 K, followed by a 30 min hold at 498 K.

2.8 Catalyst Characterization

2.8.1 X-ray Diffraction

X-ray diffraction (XRD) spectra of ground, powdered samples were obtained using either a Rigaku Miniflex 2005C103 XRD at the LSU Materials Characterization Center, or using the powder XRD beamline at the LSU Center for Advanced Microsructures and Devices, both using Cu Kα radiation. Typically these samples were scanned with a step size of 0.04°, 2-6 s integration time. Phases were identified by comparing to the ICDD database. The runs were processed using Jade to remove the background and perform K-alpha2 stripping and to smooth the signal.

2.8.2 Chemisorption

The chemisorption experiments were carried out with a Micromeritics Pulse Chemisorb 2700 fitted with a 97 µL loop. The gases used were: reduction, 10% H_2/90% N_2; analysis, CO; carrier, He. It was assumed that there was one surface metal atom per molecule of CO. The samples were first cleaned in 573 K in He for 1 h, then reduced in the N_2/H_2 for 3 h at 523 K.

2.8.3 Porosimetry

BET surface areas and pore size distributions (PSD) were obtained from N_2 adsorption/desorption isotherms using a Quantachrome AS-1, after at least 30 min of drying

under vacuum at 573 K. The PSDs were computed from the desorption branch (20 points) by the BJH algorithm.

2.8.4 Inductively Coupled Plasma – Atomic Emission Spectroscopy

Elemental analyses for Pd were by Inductively Coupled Plasma- Atomic Emission Spectroscopy (ICP-AES), after dissolving the Pd catalysts in boiling concentrated 50% HNO_3/ 50% HCl. The Pd/carbon was scraped from the monoliths, weighed and added to the acid in a water cooled glass distillation column. The mixture was boiled vigorously for >2 days to dissolve the catalyst completely, adding more acid as necessary. After dissolution DI water was added and the solution boiled in a fume hood to remove some acid gases. Then the solution was further diluted and bottled. The ICP was calibrated using a 25 ppm Pd standard.

CHAPTER 3 RESULTS AND DISCUSSION

3.1 Carbon Catalysts

The carbon loadings of the monoliths are presented in Table 3.1. All of the monoliths were prepared using the CMN-3 method, with the exception of AMM-12 and AMM-13 which were prepared without the addition of the Calgon PCB 6x16. AMM-1 to AMM-4 had too many clogged channels to be used in any experiments, and AMM-11, AMM-14 and AMM-15 were chipped during synthesis, making it impossible to determine the loading of the carbon on the monoliths and therefore also the amount of Pd present.

Additionally, some of the commercial Pd/carbon catalysts were pressed into pellets using between 50-75% Sasol Catalox Sba-90 alumina. They were pressed using water contents between 5-20%, in a stainless steel die at 267,000 N, and then dried at 373 K overnight. However, they failed to maintain mechanical strength upon use, breaking up. The eventual course of action was to put the commercial catalyst in the screen by itself, because, as it was going to slowly fall out of the screen anyway, it was better to start with 100% catalyst.

Table 3.1 Properties of carbon coatings on monoliths

Monolith	Method	Carbon Loading
AMM-5	CMN-3	6.31%
AMM-6	CMN-3	8.12%
AMM-7	CMN-3	6.03%
AMM-8	CMN-3	6.55%
AMM-9	CMN-3	12.4%
AMM-10	CMN-3	10.3%
AMM-12	No Calgon PCB	4.47%
AMM-13	No Calgon PCB	8.32%

3.2 Surface Area and Porosimetry

The N_2 porosimetry for the carbon OMC-5-1 made using method CMN-3, and ground into powder using a mortar and pestle, gave an average pore diameter of 5.5 nm, a BET surface area of 640 m^2/g, and a total pore volume of 0.51 cm^3/g for pores smaller than 29 nm diameter ($P/P_0 < 0.95$). The pore size distribution is shown in Fig. 3.1. These results compare favorably to other carbons prepared by templated sol-gel methods to give ordered mesoporous systems with hexagonal or cubic symmetry.[37]

The coating from the carbon monolith AMM-6 gave a pore distribution as shown in Fig. 3.2, with an average pore size of 9.4 nm, a BET surface area of 62 m^2/g, and a pore volume of 0.20 cm^3/g for pores smaller than 180 nm diameter ($P/P_0 = 0.99$). Therefore the carbonization of the coated monoliths proceeds differently from that of the pure mesoporous carbons, resulting in some pore closure which reduced the surface area. There was also a broader range of pore sizes – compare Fig. 3.2 to Fig. 3.1.

Sample PdP-01 is a Pd-impregnated Calgon PCB carbon ground to 120-200 mesh. The pore size distribution is displayed in Fig. 3.3, giving a BET surface area of 990 m^2/g. The average pore size is 3.5 nm with a total pore volume of 0.55 cm^3/g for pores smaller than 180 nm diameter ($P/P_0 = 0.99$).

A comparison of Figs. 3.1-3.3 shows that the Calgon is a mesoporous (dominant pore size ~4 nm), high surface area carbon that remains mostly intact when mixed with a mesoporous carbon synthesized by the resorcinol-formaldehyde (RF) polymerization method. The RF carbon is less homogeneous but with larger pore sizes (~7 nm, Fig. 3.1). When carbonized on a washcoat even larger pore sizes develop from the RF carbon, with pores between 5-12 nm. This would be expected to result in smaller intraparticle gradients during reaction.

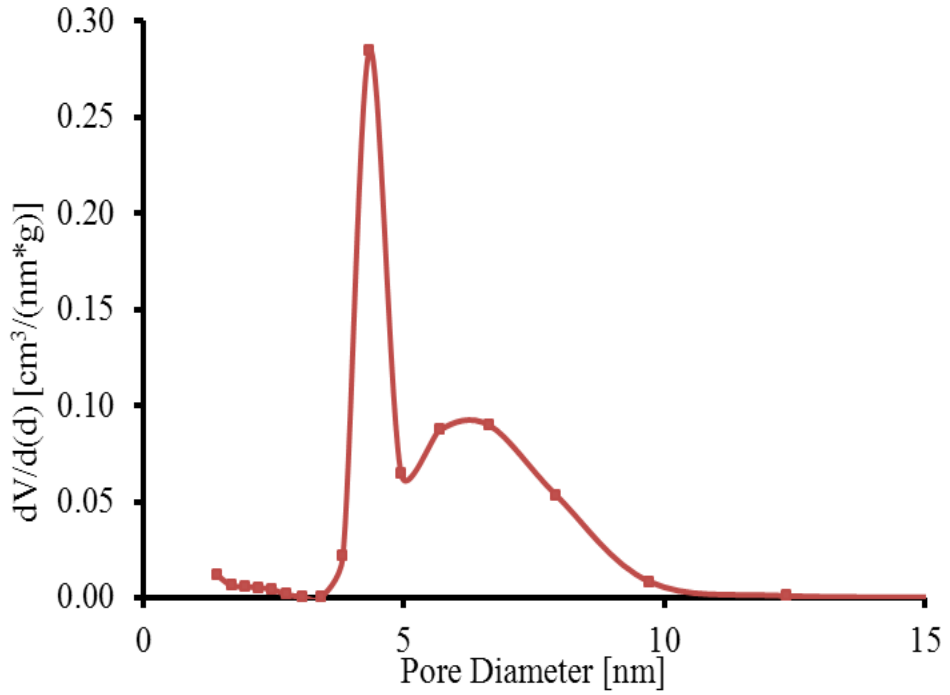

Figure 3.1 Pore size distribution by the BJH algorithm of mesoporous carbon OMC5-1

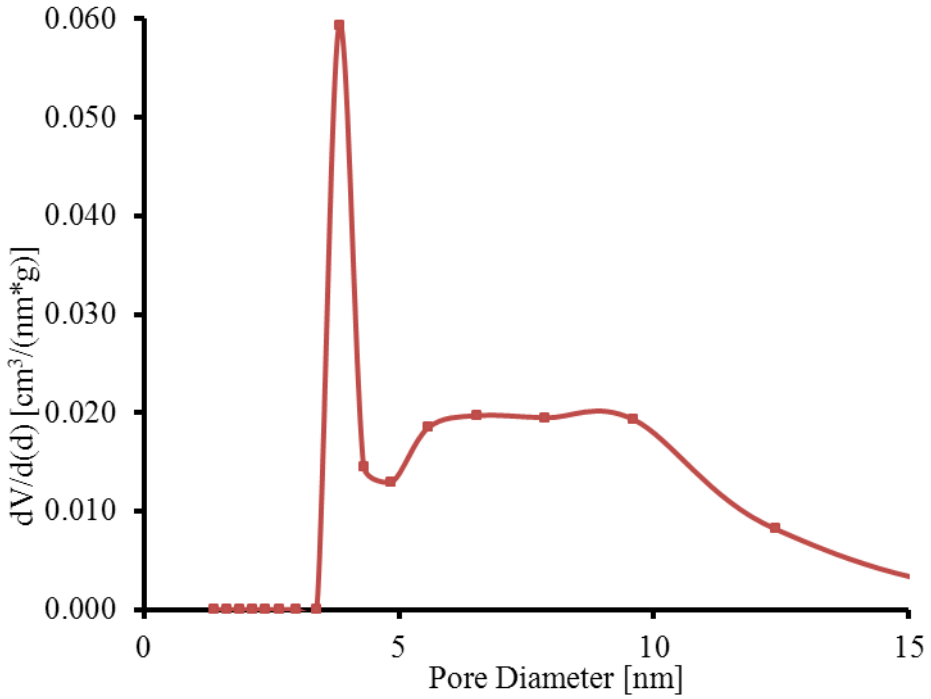

Figure 3.2 Pore size distribution by the BJH algorithm of mesoporous carbon on AMM-6

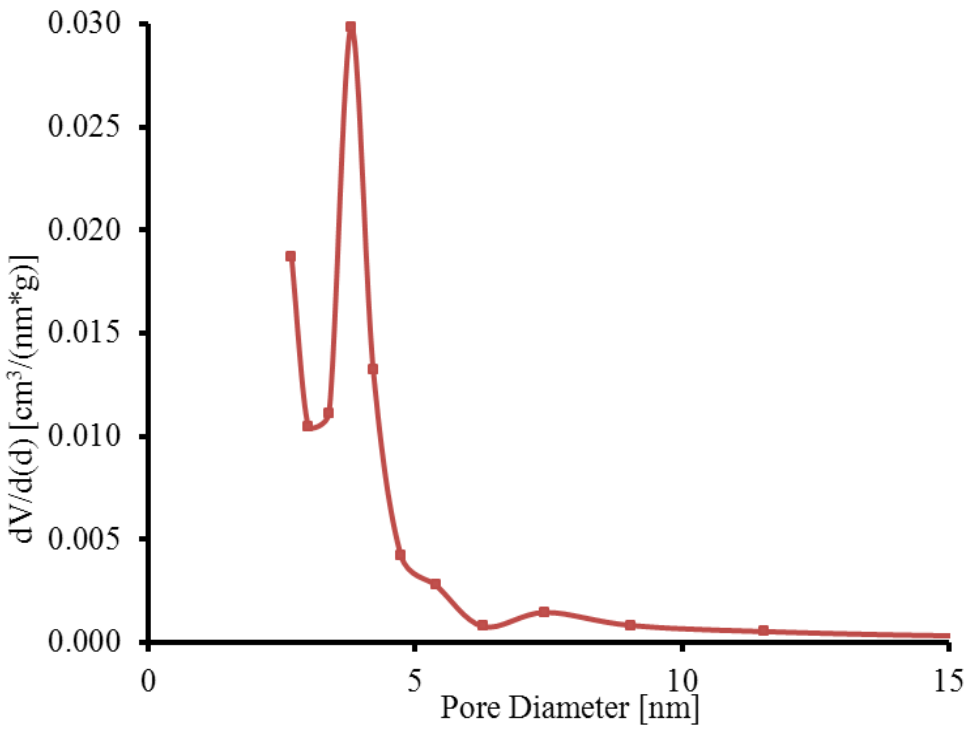

Figure 3.3 Pore size distribution by the BJH algorithm of mesoporous carbon PCB-Pd1

The pore size distribution for the "Corma" Ti-silicate is shown in Fig. 3.4. It gave an average pore diameter of 2.8 nm, a BET surface area of 750 m^2/g, and a total pore volume of 1.1 cm^3/g for pores smaller than 35 nm diameter (P/P_0 = 0.99). The BET surface area reported by Corma for this calcined synthesis is 884 m^2/g with a pore volume of 0.67 cm^3/g.[16]

The pore size distribution for the "Eimer" Ti-silicate is shown in Fig. 3.5. It gave an average pore diameter of 2.1 nm, a BET surface area of 960 m^2/g, and a total pore volume of 0.76 cm^3/g for pores smaller than 180 nm (P/P_0 = 0.99). The calcined BET surface area reported by Eimer is 1546 m^2/g at the exact same ratios of surfactant and Ti loading.[36] While both PSDs show evidence of highly uniform pores, the "Corma" synthesis is slightly better, because more uniform.

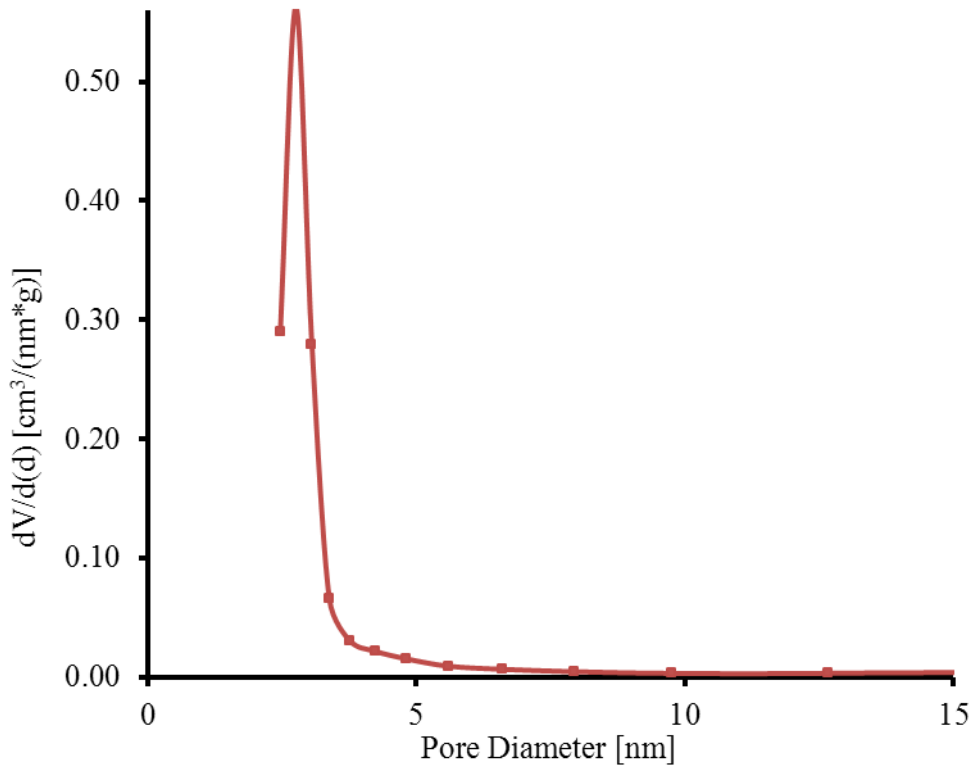

Figure 3.4 Pore size distribution by the BJH algorithm of Ti-silicate Corma Synthesis

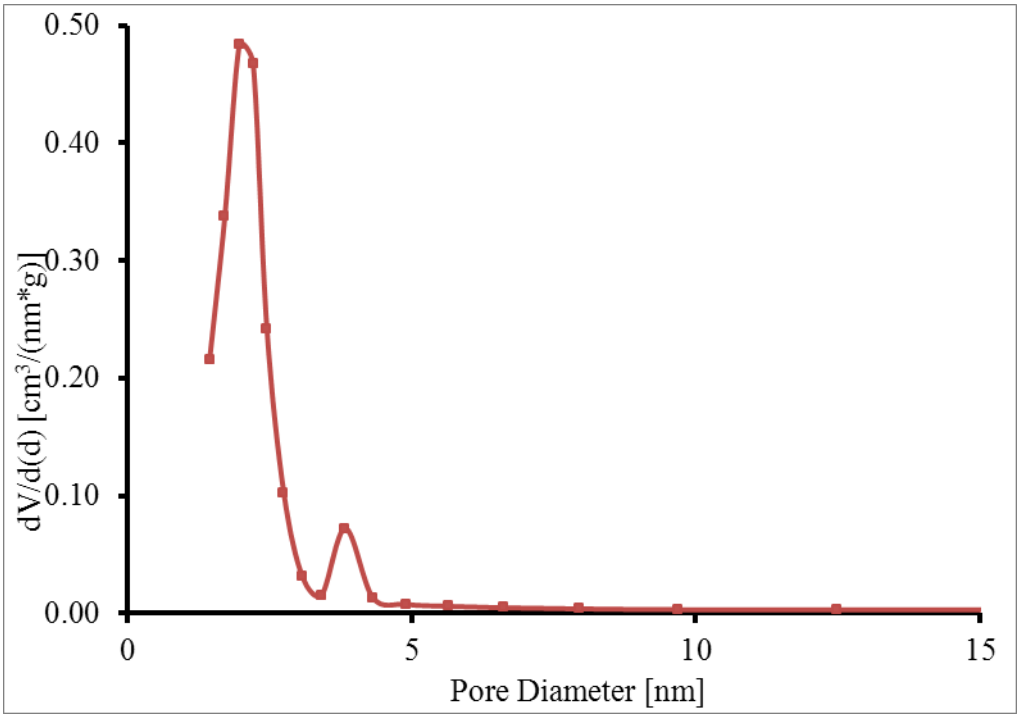

Figure 3.5 Pore size distribution by the BJH algorithm of Ti-silicate Eimer Synthesis

3.3 CO Chemisorption

Pulse CO chemisorptions were performed on several of the Pd-impregnated samples to determine their dispersions. Two runs using 0.422 g of OMC-5 catalyst were completed, both giving 19% dispersion. The impregnated Calgon carbon PdP-01 gave a dispersion of 17%, while the commercial Pd/C MPT-5 catalyst yielded a dispersion of 33%. This sample was treated slightly different from the others since it had been reduced once previously, prior to shipment. It was cleaned at 523 K for 2 h in He and reduced at 523 K for only 1 h in H_2/N_2; the more lengthy reductions of the other materials were needed to ensure maximum reduction.

3.4 Elemental Analysis

The ICP analysis for monoliths AMM-8, AMM-9 and AMM-10 after a single deposition showed that the Pd loading was only 1.2 wt%, so the deposition procedure was repeated and the second ICP analysis indicated that they had a 5.9 wt% Pd loading. ICP for catalyst PdP-01 found it to have a Pd loading of 6.2%, while for OMC-5F (the Pd-loaded OMC-5) the loading was 3.2%.

3.5 Characterization of Ti-MCM-41 Silicates by TGA and XRD

The first “Corma” and “Eimer” method syntheses were inspected by thermogravimetric analysis (TGA) to confirm that the calcination period was sufficient to remove all organic surfactant from the sample. The results showed after calcination there was no weight reduction at 723 K when exposed to air. This proved the calcination period to be adequate.

Efforts to turn these catalysts into pellets or to coat them on cordierite monoliths or alumina pellets failed. Pellets were pressed at 267,000 N in a stainless steel die at the Louisiana Transportation Research Center, and then dried at 373 K at compositions (wt. %) varying from 50/50 Ti MCM-41/ alumina (Sasol Dispal) to 80/20 Ti MCM-41/ alumina. After the pellets were

dried they failed to remain cohesive, especially when exposed to the model diesel feed. When coated onto the monoliths they could be easily removed from the surface and so could not be used in a reactor.

The XRD results from the LSU Center for Advanced Microstructure Devices (CAMD) XRD were greatly superior to those from the LSU Materials Characterization Center (MCC), because it can scan to a much lower angle without detector saturation. These XRD results were similar to those from the literature, with peak locations between 2-3º 2θ when calcined, the exact location increasing with calcination temperature/time.[16, 36] They are shown in Figs. 3.6-3.7. Note that the narrower peak for the "Corma" synthesis denotes more uniform pore wall spacing. The d-spacing was calculated using Bragg's Law, equation 1, for n = 1. The radiation wavelength λ used at CAMD is 0.152 nm.

$$2\,d\,sin\theta = n\,\lambda \quad [1]$$

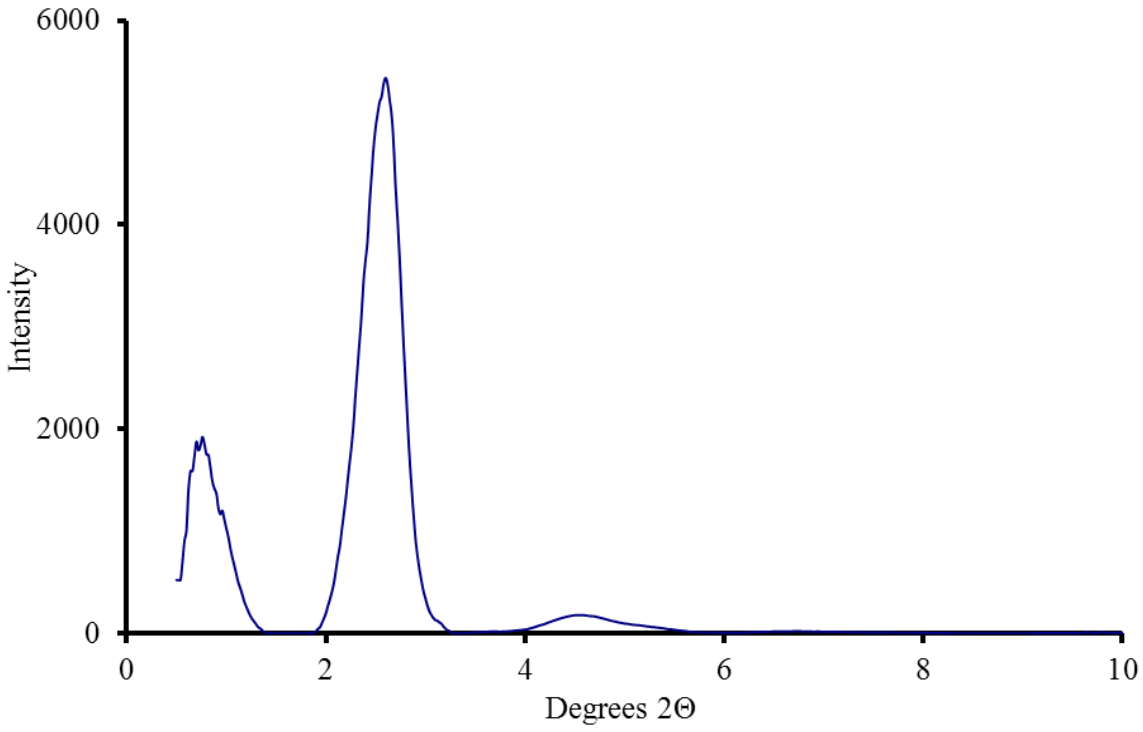

Figure 3.6 XRD pattern for Corma synthesis

The center of mass of the XRD peaks showed that the "Corma" sample's peak was centered at 2.60 degrees 2θ with a d-spacing of 3.35 nm, and the "Eimer" sample's peak was at 2.45 degrees with a d-spacing of 3.56 nm. The literature d-spacing for the calcined Corma synthesis was 2.8 nm.[16] The literature showed that the d-spacing for the calcined "Eimer" sample was 3.142 nm.[36]

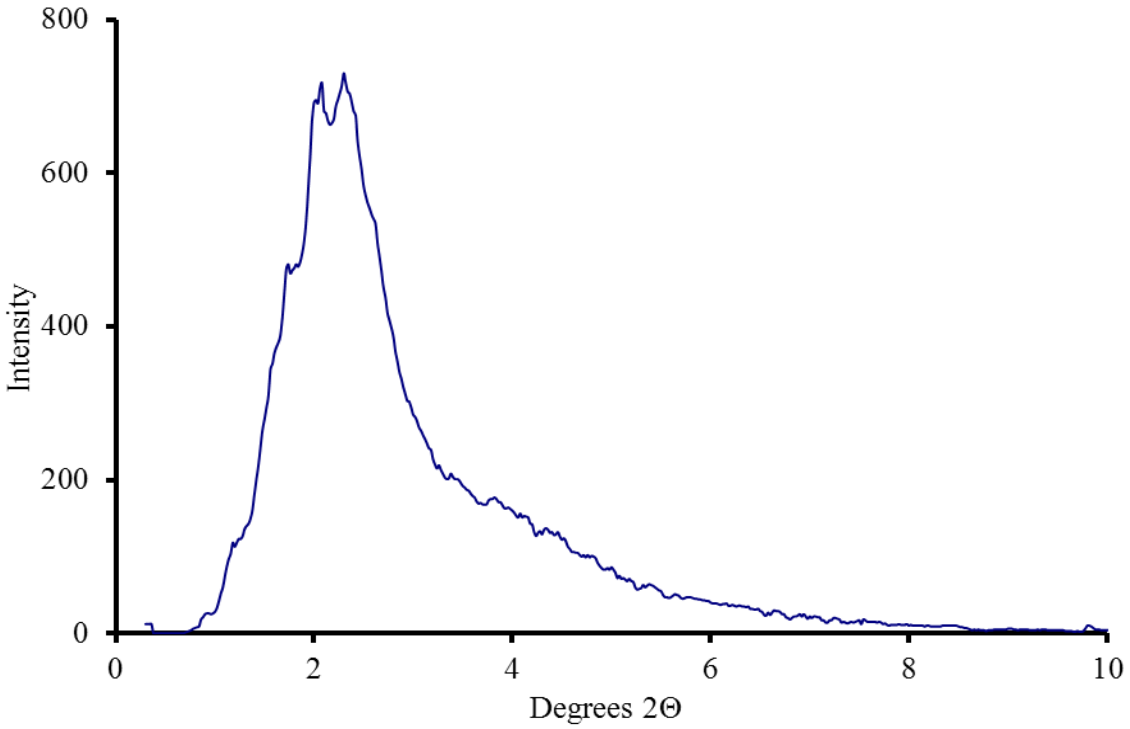

Figure 3.7 XRD pattern for Eimer synthesis

3.6 GC Results

The GC retention times for the feed compounds are shown in Table 3.2. Additionally, there was a substantial C18 impurity (from hexadecane) at about 26.3 min. The desired dibenzothiophene sulfone is located at 29.3 minutes. The small amounts of the N-compounds made them very hard to quantify, but it is unlikely they were reacting in the absence of evidence of other reactions involving the 2-methylnaphthalene, DBT, thiophene and ethylbenzene.

Table 3.2 GC retention times

Compound Name	Retention Time(min)
Thiophene	1.75
Ethylbenzene	3.25
Mesitylene	5.13
2-methylnaphthalene	14.3
Hexadecane	23.1
Dibenzothiophene	24.6
Acridine	25.1
Carbazole	25.5

3.6.1 Semibatch Rocking Reactor Results

In all of these reactions 9+ mL of the initial 10 mL liquid charge were recovered, and there was no loss of pressure by leak check prior to the experiments. The reactors were all loaded with 0.1 g of catalyst and run for 4 h. Both the "heavy" and "light" feeds were used. In many of these reactions at high conversion there was an orange solid on the catalyst, but these amounts were small compared to the liquid, so it was easier to extract and analyze this phase only in the larger volume (autoclave) runs. From Tables 3.3 and 3.4 it is apparent that some of the feed was converted in the blank run, but without the catalyst the selectivity was lower for all the runs except CDX-7(2) with 3.8% Pd loading. The function of a "good" catalyst, therefore, is to shift oxidation toward more of the thiophenic compounds. In general the carbon supported catalysts in Table 3.4 gave higher conversions than the Ti-MCM-41 catalysts, at the same temperature. Also, conversions increased with temperature, as expected, and also with O_2 pressure. The Ti-MCM-41 and Pd/C catalysts all showed selectivities > 10% at 363 K and 1.13 MPa O_2.

The rocking reactor runs have a margin for error in the conversion of ethylbenzene, methyl naphthalene, thiophene and DBT of approximately 3% based on repeat GC analyses. The acridine and carbazole, only 0.02 and 0.03 wt% of the feed, respectively, gave very high standard deviations for conversion. These results are not therefore reported in Tables 3.3 and 3.4, but it was clear that they also were oxidized at <100% conversion. The Ti-MCM-41 based catalysts did a better job converting acridine, while the supported Pd converted more carbazole. Acridine is a basic N-compound, and since the sites on Ti-MCM-41 are acidic, there is stronger adsorption of acridine, allowing for the increased activity. The carbons are less acidic, with MPT-5 even being slightly basic;[1] this allows them to adsorb more carbazole, which is a more neutral compound.

The light feed resulted in higher selectivity for all catalysts and for the blank than the heavy feed. This result could be biased by some evaporation of thiophene during the experiment; thiophene was the lightest component. The "light" feed showed higher conversions with the Ti-MCM-41 catalysts, but the "heavy" feed showed higher conversions with the Pd/C catalysts showed higher conversions.

Table 3.3 Rocking reactor runs with Ti-MCM-41 Catalyst, 4 h, 10 mL

Catalyst	Feed	Conditions	Conv EB	Conv MN	Conv THIO	Conv DBT	Selectivity Mol S/Mol Arom
Blank	Heavy	90°C, 0.92 MPa	-	4.1%	-	4.2%	0.031
Blank	Heavy	90°C, 1.13 MPa	-	11%	-	24%	0.067
Blank	Light	90°C, 1.13 MPa	9.5%	5.3%	25%	8.5%	0.095
"Corma"	Heavy	70°C, 1.13 MPa	-	4.6%	-	4.0%	0.027
"Corma"	Heavy	90°C, 1.13 MPa	-	12%	-	24%	0.061
"Corma"	Light	90°C, 1.13 MPa	0.76%	3.1%	9.1%	2.1%	0.13
"Corma"	Light	90°C, 1.13 MPa	9.1%	5.2%	42%	6.8%	0.15
"Eimer"	Heavy	70°C, 1.13 MPa	-	4.3%	-	4.9%	0.035
"Eimer"	Heavy	90°C, 1.13 MPa	-	11%	-	25%	0.070
"Eimer"	Light	90°C, 1.13 MPa	12%	4.0%	42%	3.5%	0.12

Table 3.4 Rocking reactor runs with Pd/C catalysts, 4 h, 10 mL

Catalyst	Feed	Conditions	Conv EB	Conv MN	Conv THIO	Conv DBT	Selectivity Mol S/Mol Arom
Blank	Heavy	90°C, 0.92 MPa	-	4.1%	-	4.2%	0.031
Blank	Heavy	90°C, 1.13 MPa	-	11%	-	24%	0.067
Blank	Light	90°C, 1.13 MPa	9.5%	5.3%	25%	8.5%	0.095
Pd/MPT-5	Heavy	70°C, 1.13 MPa	-	3.8%	-	6.1%	0.049
Pd/MPT-5	Light	90°C, 1.13 MPa	0.01%	3.0%	12%	9.4%	0.33
Pd/D	Heavy	70°C, 1.13 MPa	-	3.8%	-	6.1%	0.049
Pd/D	Heavy	90°C, 0.92 MPa	-	39%	-	41%	0.032
Pd/D	Heavy	90°C, 1.13 MPa	-	13%	-	26%	0.061
Pd/D	Heavy	90°C, 0.92 MPa	-	47%	-	62%	0.040
Pd/D	Light	90°C, 0.92 MPa	-	25%	-	45%	0.055
Pd/D	Light	90°C, 1.13 MPa	8.9%	2.4%	50%	8.6%	0.22
Pd/D	Light	90°C, 1.13 MPa	7.2%	1.9%	27%	19%	0.19
CDX-7(2)	Heavy	90°C, 1.13 MPa	-	13%	-	28%	0.066
CDX-7(2)	Heavy	90°C, 0.92 MPa	-	27%		46%	0.052
CDX-7(2)	Light	90°C, 1.13 MPa	8.0%	39%	16%	14%	0.028
Pd/E	Heavy	90°C, 1.13 MPa	-	12%	-	28%	0.071
Pd/E	Heavy	90°C, 0.92 MPa	-	25%	-	43%	0.053
Pd/E	Light	90°C, 1.13 MPa	11.6%	7.9%	45%	12%	0.13

3.6.2 Results for Autoclave Reactors

The problems inherent in the rocking reactor experiments (small size, high solid surface/volume ratio, little solid product to analyze, hard to get exact liquid volumes after reaction) prompted additional batch runs in a stirred autoclave. It was also easier to seal the autoclave in longer-term runs. There were three autoclave runs with catalyst (a Ti-MCM-41, a Pd/C, and a typical homogeneous oxidation catalyst) and O_2 as oxidant. The O_2 supplied to the system was fixed, by using the empty volume and the ideal gas law it is estimated that there was 1 mol O_2/ 4 mols reagent. There was additionally a run with a catalyst (a Pd/C) and benzoyl peroxide oxidant, 1 mol peroxy groups/ 5 mols reagent under N_2 pressure. The Ti-MCM-41 and Pd/C catalysts were chosen based on their selectivities in the rocking reactor runs. Typical

conditions (except where noted) were “light” feed, 100 mL/g feed/total catalyst ratio, 1.13 MPa O_2, 363 K. For the homogeneous cobalt octoate catalyst the feed/catalyst ratio was scaled to the same molar ratio (0.0049 moles Pd/ L feed) as for the Pd runs, which gave 1.04 g of 6% Co with octoate ligands in methanol. The results in Table 3.5 were computed based on initial activity over the first 4 h of the run for AC-01 and AC-03 but AC-02 is computed from 24 h data, because no 4 h data were available.

Table 3.5 TOF(s^{-1}), total metal site basis, and autoclave selectivity (mol. S/ mol. aromatic)

	AC-01	AC-02	AC-03	AC-04
Catalyst	“Eimer”	Pd/E	Co Octoate	Pd/E(peroxide)
EB(TOF)	3.7 E-03	9.7 E-04	6.1 E-04	4.1E-04
MN(TOF)	1.6 E-03	0	7.2 E-06	4.3E-04
DBT(TOF)	8.2 E-05	0	8.6 E-07	2.1E-05
THIO(TOF)	5.1 E-04	1.9 E-04	5.0 E-05	-
N-comps.(TOF)	1.6 E-05	2.7 E-06	1.3 E-05	5. 1E-04
Selectivity	0.095	0.073	0.11	-

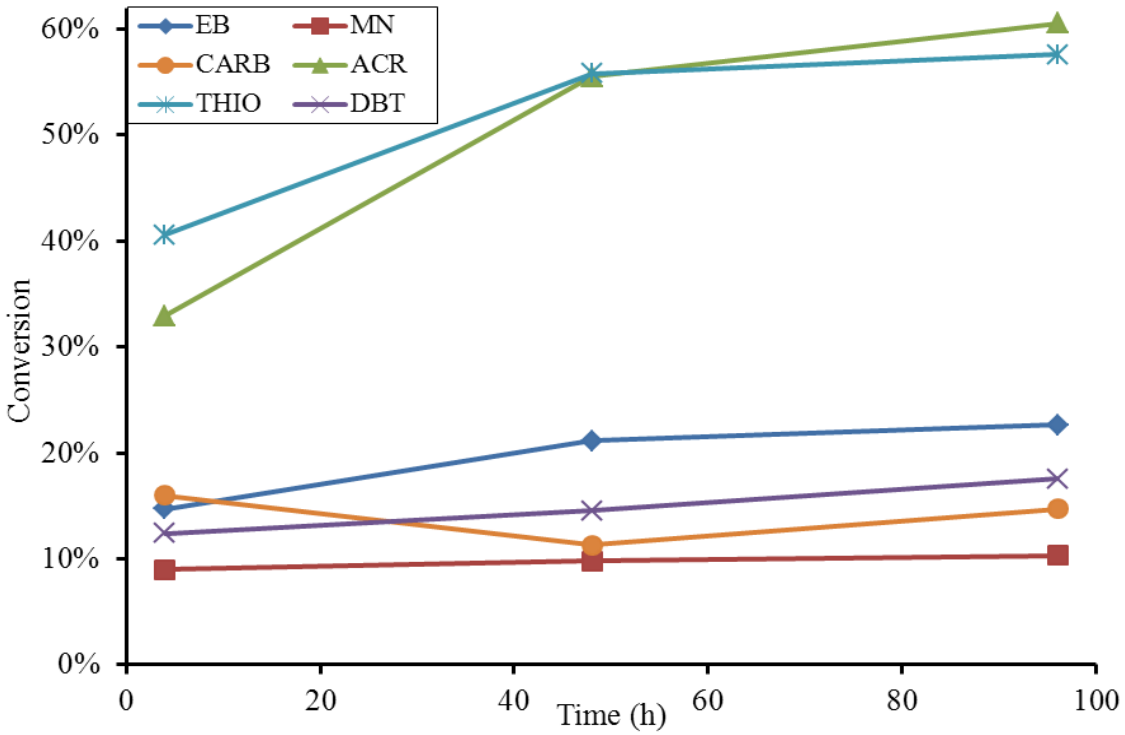

Figure 3.8 Conversions for run AC-01, "light" feed with "Eimer" Ti-MCM-41 catalyst

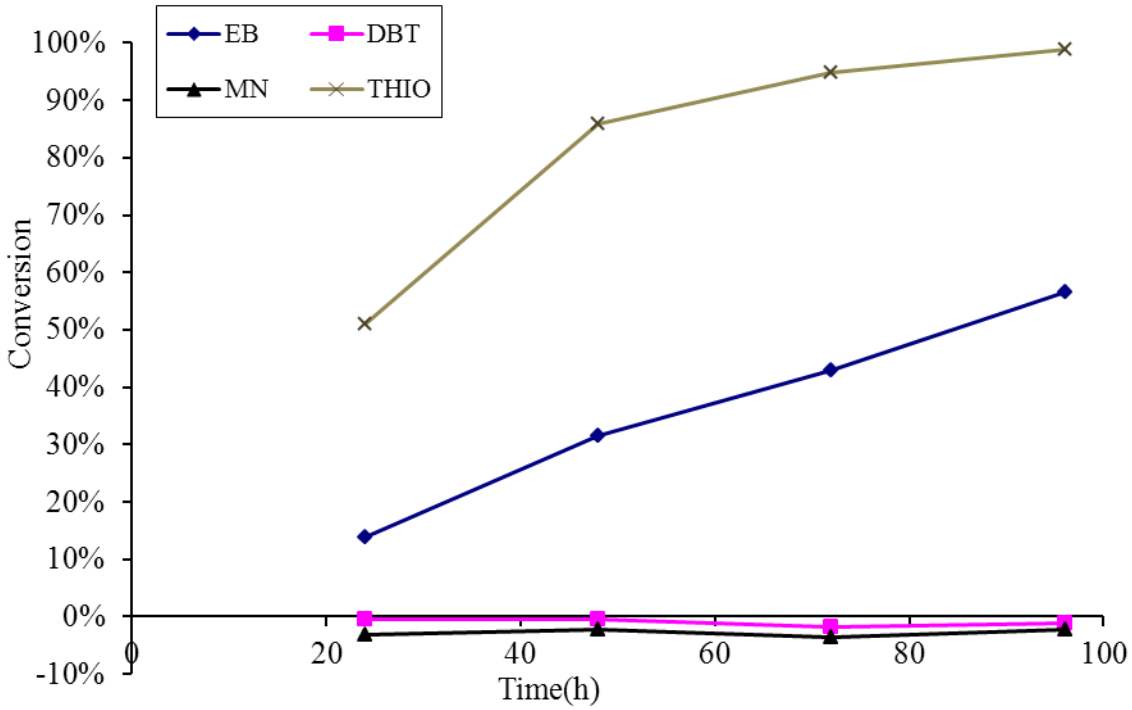

Figure 3.9 Conversions for run AC-02, catalyst Pd/E, 363 K, and 1.13 MPa

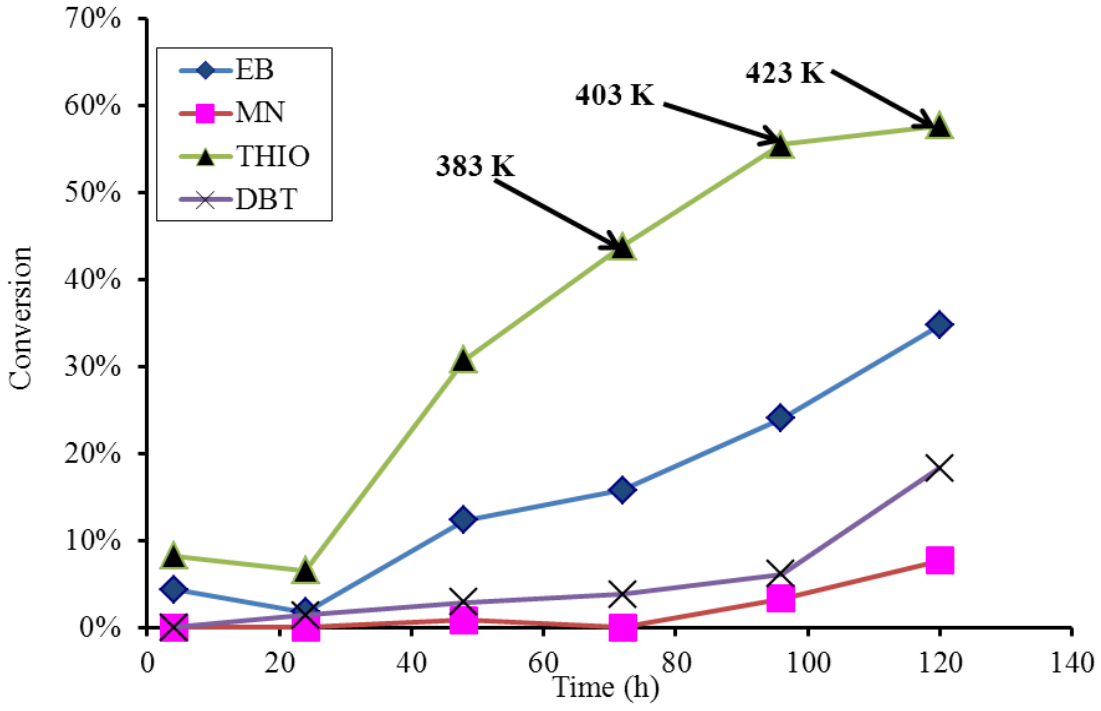

Figure 3.10 Run AC-03. The temperature was ramped after starting at 363 K for 48 h, to 383 K for 24 h, to 403 K for 24 h and finally 423 K for 24 h

Run AC-01 ("Eimer" Ti-MCM-41) resulted in high conversions for only thiophene and acridine. The data are plotted in Fig. 3.8, and it is obvious that after 48 h very little happened, either due to product inhibition or catalyst deactivation, or both. This run showed high initial activity both for the aromatics and the sulfur heterocycles, but there were almost no differences in catalyst activity for the N- heterocycles, for all of the catalysts. This is shown in Table 3.5, where it can be seen that the Eimer catalyst even at 24 hours has more than 5x higher TOF for the aromatics and 3x higher for the sulfur compounds than the Pd/E. But Fig. 3.9 shows that the overall conversion with the Pd is higher, likely due to more poisoning of the Ti-MCM-41 catalysts.

AC-03 was different from the other tests because it used a cobalt "metal soap" instead of a supported catalyst, and also the temperature was changed during the run. It was evident that as the temperature increased the selectivity decreased (Table 3.6). But while the cobalt octoate was initially the least active catalyst, it was the most selective at 363 K. Its data are plotted in Fig. 3.10, and the components that were not plotted did not have meaningful conversion values.

Table 3.6 Run AC-03, selectivity (mol S/ mol arom.) with respect to temperature

Temperature, K	363	383	403	423
Time, h	48	72	96	120
selectivity	0.11	0.12	0.094	0.072

Run AC-04 was conducted at 1.13 MPa N_2, a feed/catalyst ratio of 100, 363 K for 48 h, with 7 g of benzoyl peroxide which is a 0.2 peroxy group/ reagent ratio, and is plotted in Fig. 3.11. As benzene is a product of the decomposition of benzoyl peroxide, and as it was impossible to completely separate the thiophene from the benzene, the thiophene conversions are not reported here. Assuming all of the benzoyl peroxide decomposes to give benzene as a product, there would be approximately 4.5 g in the 225 mL sample, which calculates to roughly a

4 to 1 ratio in electrons (benzene/thiophene). The MS results of AC-4 at 48 h showed the electron ratio for the parent ions to actually be approximately 3 to 1, which shows that while not all benzoyl peroxide may have decomposed to benzene, much of it did. In the GC runs the benzene/thiophene peak area tripled after the addition of the benzoyl peroxide, suggesting the same conclusion.

Nothing happened after 24 h, possibly because the peroxide was used up (all peroxide molecules do not necessarily decompose to give a peroxy radical), but also there could have been the same product inhibition observed in other runs. It was not possible to calculate the selectivity for this run because of the false reading on the thiophene, but the low conversions of DBT suggest it was not high. The most important findings are in Table 5, where it is seen that the TOFs are not much greater with the benzoyl peroxide oxidant, compared to O_2.

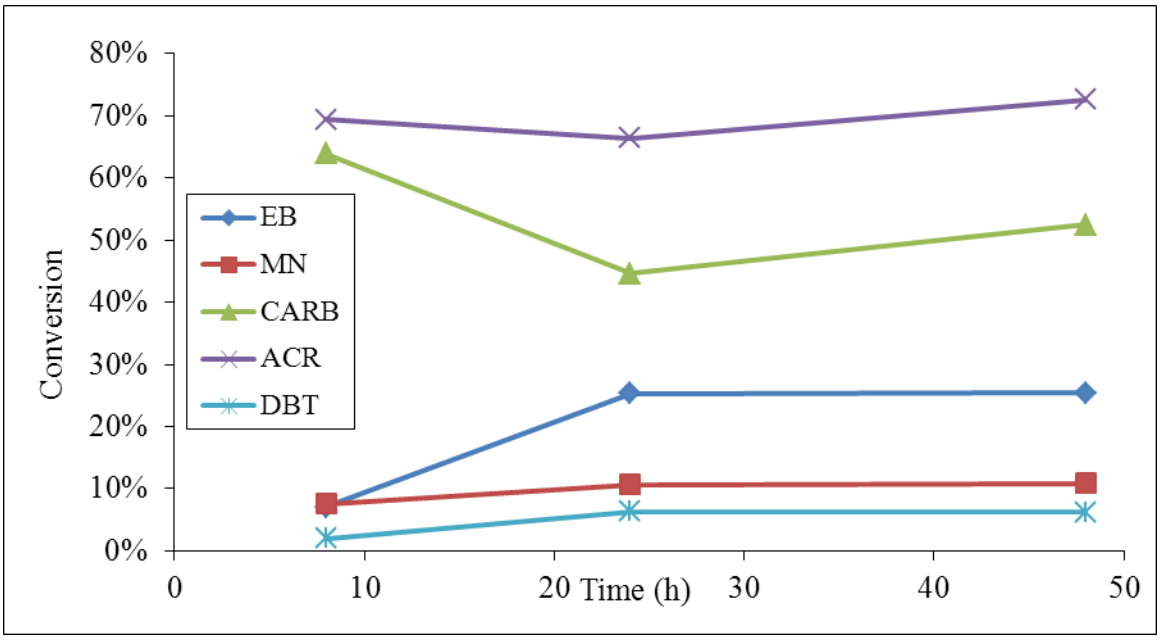

Figure 3.11 Conversions for run AC-04, catalyst Pd/E and peroxide oxidant

Some of the rocking reactor runs in 4 h achieved the same conversions as in the larger autoclave, in far less time. In theory, the results from the autoclave and rocking reactors should be similar if none of the reactions were mass transfer limited in the liquid phase and if they were

zero order in O_2. While the autoclaves could be stirred at a faster rate, the small volumes, extreme action and infinite supply of O_2 characteristic of the rocking reactors probably resulted in higher O_2 concentrations in the liquid and better O_2 contact with the catalyst.

3.6.3 POMR Results

Several blank runs were made with just feed and no catalyst show that there was no significant conversion over a few h at 1.13 MPa O_2, 343 K, 5 Hz. Run PDM-1 was conducted at the same conditions but with the "heavy" feed and loaded with monoliths AMM-8, 9, and 10 (5.9% Pd loading). However, this run had to be terminated after 1.5 h because the breaker powering the oscillating piston tripped. The reactor was not reloaded with a new feed and catalyst, and run PDM-2 was conducted at the same conditions for 6 h. In Fig. 3.12 is the conversions are plotted. There was no reaction observed past 3 h. The TOFs in Table 3.7 were computed with the 1.5-4.5 hour samples.

Table 3.7 TOF(s^{-1}), total metal site basis, and POMR selectivity (mol. S/ mol. aromatic)

	PDM-02[1]	FD401	PDM-6
Catalyst	Monolith Pd	PdP-001 Pd/C powder	Monolith Pd w/ peroxide
EB(TOF)	-	2.0E-02	8.2E-03
MN(TOF)	1.9E-02	0	5.0E-03
DBT(TOF)	7.4E-04	0	2.2E-05
THIO(TOF)	-	1.3E-02	1.3E-03
N-comps.(TOF)	6.6E-05	5.1E-05	-
Selectivity	0.030	0.061	0.078

[1]Used the heavy feed

Run PDM-3 was conducted at similar conditions with the same catalyst except the frequency was 15 Hz. There was no perceivable conversion so it appeared that again there was product inhibition or the catalyst had deactivated.

Run Fd401, was conducted at the same conditions as PDM-02 using 2.3 g of PdP-001(6.2% Pd loading) with 700 mL of "light" feed; overall there is less Pd here than for the

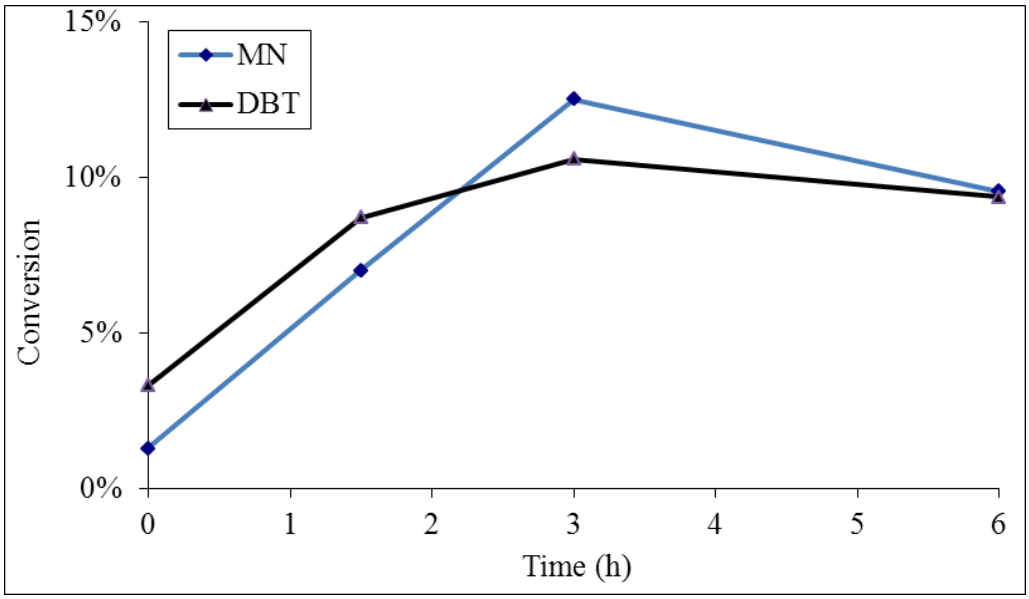

Figure 3.12 Run PDM-2 conversions

monolith runs, because while the loadings are roughly the same, 6.2 and 5.9%, there is 7.8 g of carbon on the monoliths and only 2.3 g in the screens, a 320% difference. The data for the run are plotted in Fig. 3.13 and the TOFs are in Table 3.7. This run gave the highest oxidation activity for the alkylaromatics, but there was no observed conversion of DBT, but 27% of thiophene.

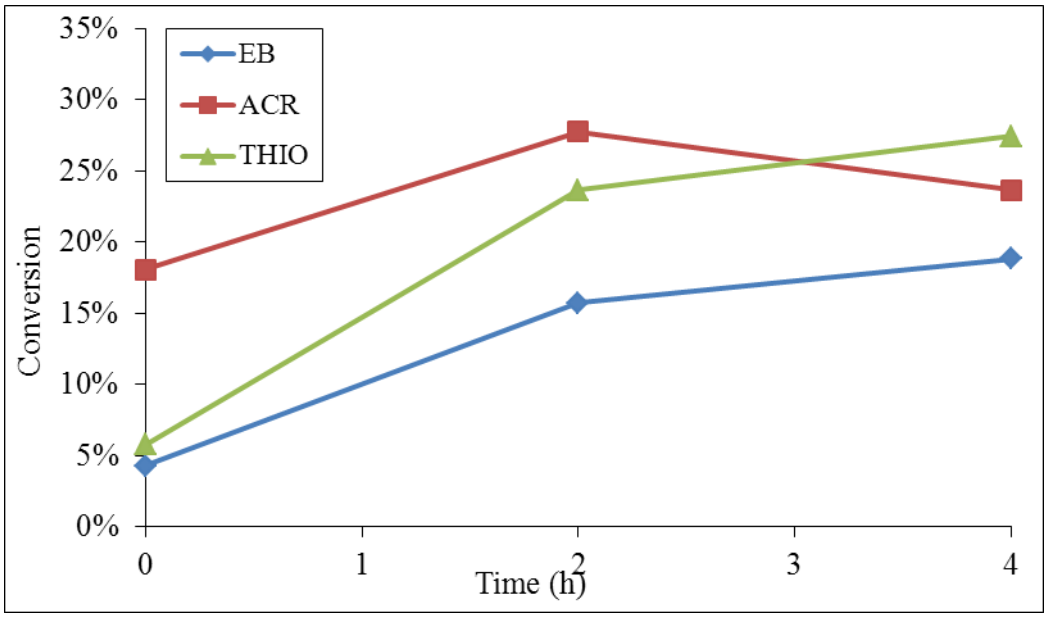

Figure 3.13 Run FD401 conversions

Finally, Run PDM-6 was conducted at 363 K and 1.13 MPa at 5 Hz, with a peroxide/reagent ratio of 0.2. The reaction progress is given in Fig. 3.14. The high conversions quickly made it impossible to quantify the small N-compound peaks, because they were obscured by product peaks, so they are not included. The conversion at 0 h was plotted because this does not include the 1 h used to heat the reactor to the final temperature, which for this run accomplished some conversion. There was no DBT conversion, but there was a large thiophene conversion. It does not appear that vaporization was a problem, because over the course of the experiment there was only moderate change in the composition of the other light compound ethylbenzene. The TOF's of the reactors without the peroxide actually gave higher TOF's and the only run that accomplished DBT conversion was the Pd monolith run without the peroxide. The TOF's are better across the board than the autoclave results, but the selectivities are worse, with the exception of the peroxide runs, in which they are equivalent.

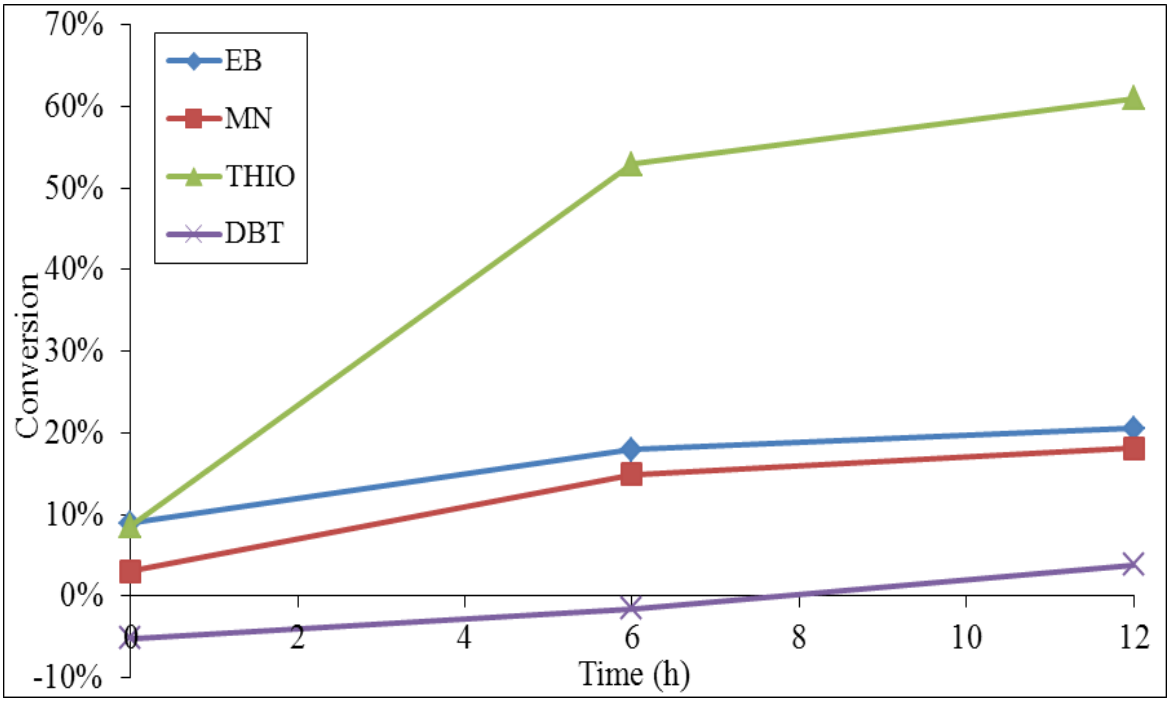

Figure 3.14 PDM-6 conversion values

3.7 Product Extractions from Catalysts

It was noted that for some of the runs there was a red to orange solid on the catalyst after the run. These were solid products from the reaction. A sample of spent catalyst was boiled in several different solvents in order to determine the solid's composition. Dichloromethane (Aldrich, >99.9%), acetone (Fisher, >99.9%), and 1:1 volume ratio ethanol/H_2O (ethanol was Aaper absolute) were all used as solvents; acetone extracted the most material based on change in color, to orange-brown. Therefore the spent catalysts were extracted with acetone under reflux for 8 h. The extracts were bottled and stored for GC/MS analysis.

3.8 Gas Chromatography/Mass Spectrometry Results

The GC/MS could identify products in the liquid phase only if the reaction gave high conversions. It was easier to identify products from the acetone extracts of the catalysts. The orange-red solid product was especially visible on the initially white "Eimer" Ti-silicalite, even in the rocking reactor runs. The best MS results were from analysis of the extracts from autoclave runs AC-01 ("Eimer" catalyst) and AC-02 (Pd/E), the 383 K and 403 K samples from run AC-03 (cobalt octoate) and the non-extract samples from run PDM-2 (5.9% Pd/C/monoliths) in the POMR. The retention times for the components of the feed and one persistent product are listed in Table 3.8.

Table 3.8 GC/MS retention times

Compound Name	Retention Time(min)
Benzene	4.5
Thiophene	4.6
Ethylbenzene	11.7
Mesitylene	15.9
Carbazole	27.1
Methylnaphthalene	28.2
Hexadecane	41.1

The structures of the feed components are shown with their molecular weights in Table 3.9, and the products and their molecular weights are shown in Table 3.10. Thiophene could not be separated from the solvent in the GC-MS, and none of its products were seen. It is probable that since thiophene's sulfone has MW = 120, which is the same MW as acetophenone, and its sulfoxide has MW = 104, which is a common ion in many hydrocarbons, that it is not be easy to find. The carbazole or acridine were not visible all the time, but that is to be expected given how little of them were used, and the fact that they could be mostly in the liquid product rather than the extracts.

There was also one unidentifiable peak at MW=160 which according to the library could be any of three possibilities shown in Table 3.11. This peak was found in most of the MS analyses.

The Run AC-01 extracts showed products BPN, OPB, PPB, IND, ACP, MBM, NCA, DBP, DBTS1 and DBTS2. There was a fairly large amount of OPB and also PPB, polymerization products of ethylbenzene. Additionally, ethylbenzene products ACP, MBM, and DBP were found in large quantities. This agrees with the results from the GC that show ethylbenzene behaving as the most reactive of the major compounds included in the feed. The NCA and BPP are from methylnaphthalene, while the IND is from the carbazole. Finally, the DBTS1 and DBTS2 are the desired sulfones and sulfoxides.

Run AC-02 extracts contained products ACP, MBM, NCA, DBP, BPP, MQA, DBTS1, DBTS2. Again, the GC results showed that ethylbenzene was the most reactive species in the feed, and the presence of ACP, MBM, and DBP in relatively large amounts supported that conclusion.

Table 3.9 Feed components and structures

Compound	Molecular Weight (g mol^{-1})	Structure
Benzene	78	C_6H_6
Thiophene	84	
Ethylbenzene	106	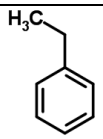
Mesitylene	120	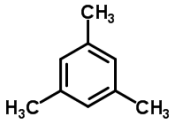
Carbazole	167	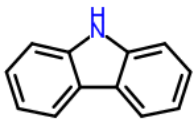
Acridine	179	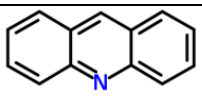
Dibenzothiophene	184	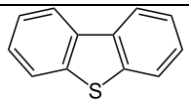
Methylnaphthalene	142	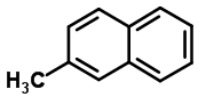
Hexadecane	226	$C_{16}H_{34}$
Benzoyl Peroxide	242	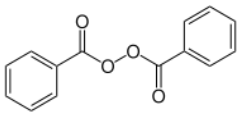

Table 3.10 Oxidation products identified by GC/MS

Compound	MW (g mol^{-1})	CAS #	Acronym	Structure
Acetophenone	120	000-098-86-2	ACP	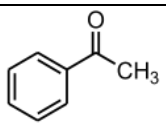
Benzenemethanol, α-methyl	122	000-098-85-1	MBM	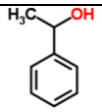
1-naphthalene carboxaldehyde	156	000-066-99-9	NCA	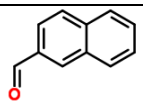
5H-indeno(1,2-b)pyridine	167	000-244-99-5	IPY	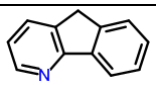
Benzenpropanenitrile	131	000-645-59-0	BPN	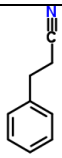
2,5-Dimethyl-3-isopropylpyrazine	150	013-610-20-3	DIP	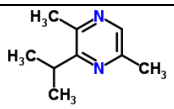
Benzene, 1,1'-oxybis[3-phenoxy-]	354	000-748-30-1	OPB	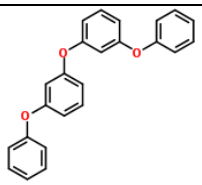
Benzene, 1,1'-oxybis[4-phenoxy-]	354	003379-41-7	OPB	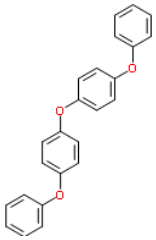
Benzene, 1,3-bis[3-phenoxy-phenoxy]	446	002-455-71-2	PPB	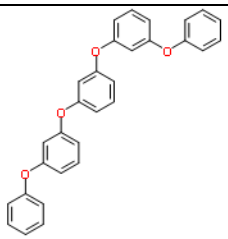
2H,8H-benzo[1,2-b:5,4-b']dipyran-10-propanol	330	026-535-37-5	BPP	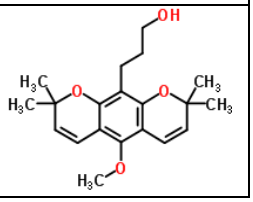

(Table 3.10 Continued)

Compound	MW(g mol^{-1})	CAS #	Acronym	Structure
2,4-bis(dimethylbenzyl) -6-t-butylphenol	386		DBP	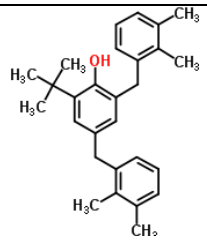
Dibenzothiophene sulfoxide	200	001-013-23-6	DBTS1	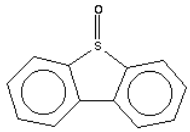
Dibenzothiophene sulfone	216	001-013-23-6	DBTS2	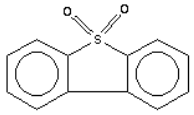
Benzo(h)quinoline	179	000-230-27-3	BQN	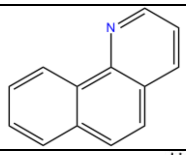
Indole	117	120-72-9	IND	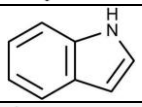
2-methylbenzothiophene	148	1195-14-8	MBT	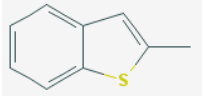
3,5 pyridinedicarboxylic acid, 1,4-dihydro, 2,6 dimethyl,diethyl ester	253	1149-23-1	PCA	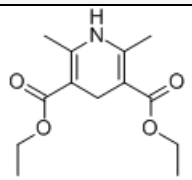

Table 3.11 Possibilities for the peak at MW = 160

Substance	CAS #	Acronym	Structure
4-methyl,1-oxide quinazoline	10501-56-1	MQO	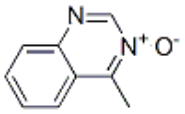
4(3H)-quinazolinone	2436-66-0	MQA	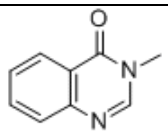
1,3-naphthalenediol	92-44-4	NDL	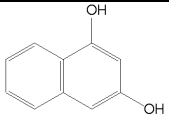

The run AC-03 non-extract samples showed products ACP, MBM, BPN, NCA. For the autoclave runs only the extract samples showed products in identifiable amounts, except for run AC-03 where data were also collected at 383 K and 403 K. No sulfur derivatives were observed.

The workup on the 4.5 h sample of Run PDM-2 revealed MBT, which is a product of DBT. PCA, a product of acridine, was also observed, along with BQN and IND, products of carbazole.

3.9 FTIR Analysis

The oxidation products of primary interest were aldehydes, ketones, carboxylic acids, sulfones, and sulfoxides. The pure solvent peaks were identified by matching to spectra from the NIST database or the Sigma-Aldrich database, and these standard spectra matched the measured FTIR results.[38] The peaks indicative of aryl sulfones are located at 650, 1165 and 1365-1380 cm^{-1}, while for an aryl sulfoxide there is a peak at 1035-1045 cm^{-1}. The samples confirmed the GC/MS results showing the presence of aryl sulfones and sulfoxides in both the liquid product samples and the acetone extracts of the catalysts. In agreement with previous work, it appears as if much of the sulfone remained with the catalyst.[7, 16]

In Fig. 3.15 spectrum A is pure hexadecane, spectra B and C are duplicate samples of hexadecane spiked with DBT sulfone. During sample preparation 1.5 mL was dosed with 0.1 g DBT sulfone, the container was sealed and exposed to mild heating until the DBT sulfone powder was no longer visible. When the sample was cooled the sulfone reprecipitated in the container, showing that there is not a high solubility of sulfone in the hexadecane. Referring back to the GC results of a similar standard it was noted that the sulfone peak, while observable in pure hexadecane, was small, on the same order of magnitude as the nitrogen compounds. Examening the common ranges for aryl sulfone peaks it was determined that the largest peak

appearing at 1365-1380 cm^{-1} is obscured by a large C-H peak from the hexadecane. There were also no perceivable peaks at 650 or 1165 cm^{-1}. Therefore it is likely that with a hexadecane solvent it is not possible to see DBT sulfone by FTIR.

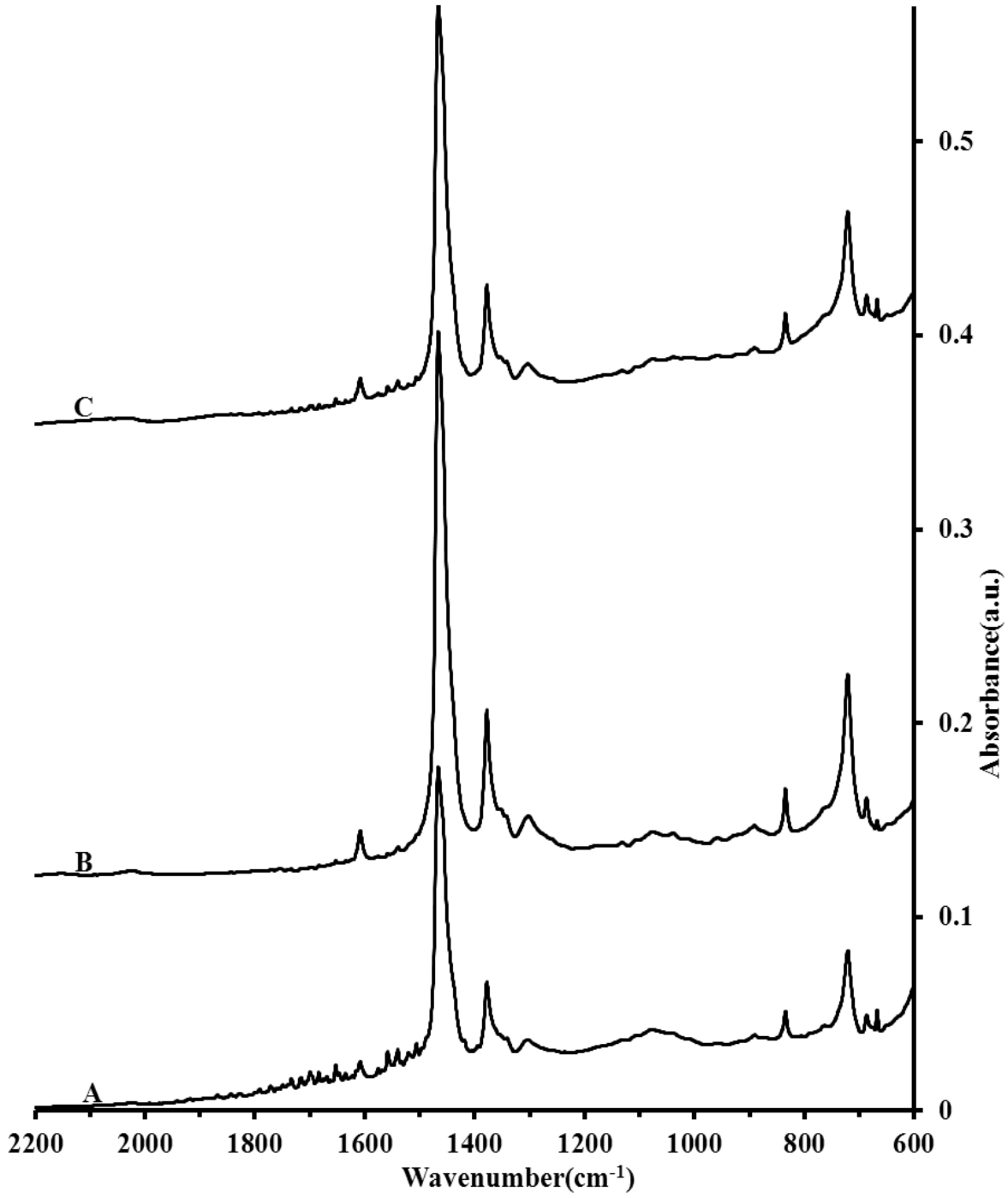

Figure 3.15 FTIR spectra, where A is hexadecane, B and C are spiked with DBT sulfone

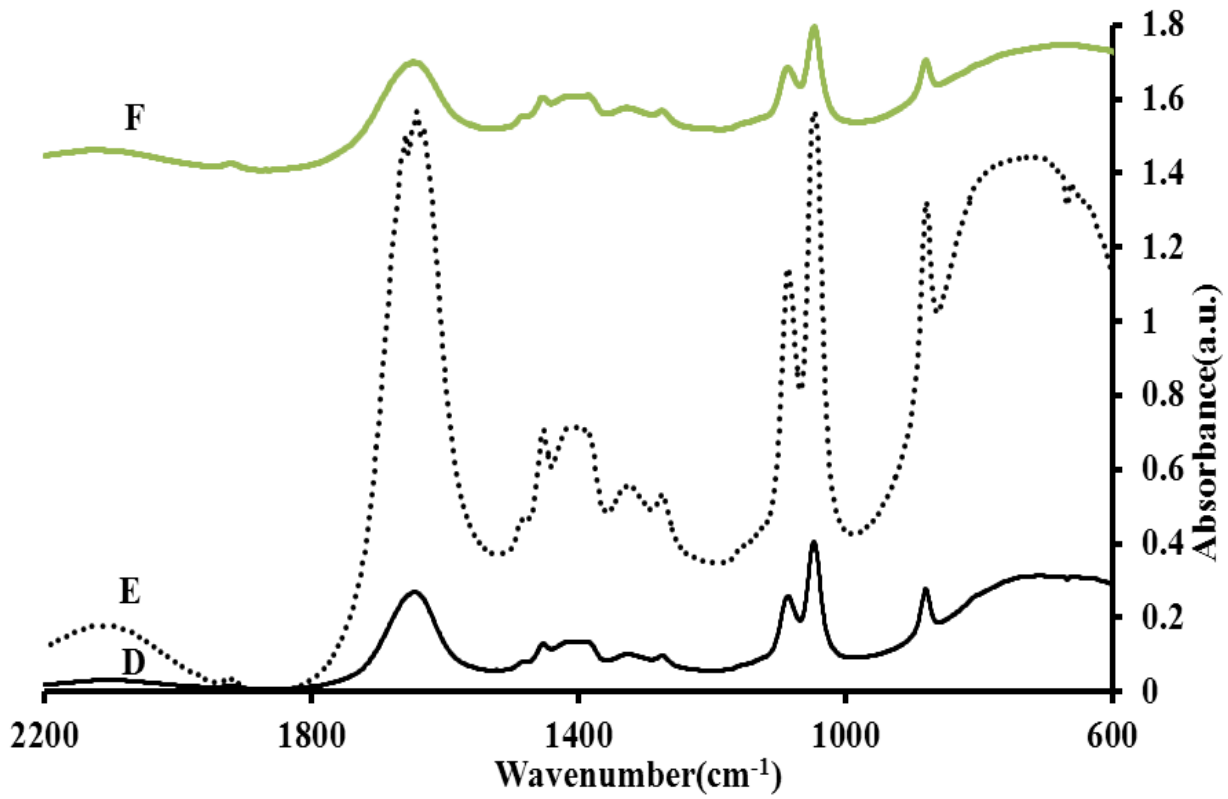

Figure 3.16 FTIR spectra of 50/50 H_2O and ethanol extracts. E is the solvent before extraction, D and F are AC-01 extracts

Fig. 3.16 shows the FTIR spectra from the 50/50 ethanol/ water extractions. Spectrum E is for the ethanol/water solvent while spectra D and F are for the extracts from the "Eimer" Ti-MCM-41 catalyst used in run AC-01. The range to find the carbonyl groups in the products was obscured by the wide scissors vibration of H_2O. Neither the sulfoxide or sulfone peaks are visible in these spectra. There is also no indication of any other product. The MS results from this solvent showed that it was not as effective as acetone, and as the analysis of the acetone extracts produced abundant data on product identities, this FTIR work was not continued.

Fig. 3.17 shows the spectra for the dichloromethane(DCM) extract of the Pd/E catalyst used in run AC-02. Spectrum G is pure DCM, while spectrum H is the extract. Spectrum G was compared to the literature and found to be comparable for pure DCM over the measured range. The first observable product in spectrum H is the peak of for water at 1600 cm^{-1}. The 1460 cm^{-1}

and 1375 cm^{-1} peaks are of the same shape and at the same location as the hexadecane standard's C-H peaks. The 1375 cm^{-1} peak obscures the sulfone peak. At 650 cm^{-1} there is a peak that corresponds to the lowest frequency sulfone peak. At 1165 cm^{-1} there is a small shoulder on the much larger peak that is characteristic of both DBT and its oxidation products; the shoulder corresponds to sulfone. There could be some products in the carboyl range but it is hard to tell whether there is background or just very small peaks. There is no way to see the sulfoxide peak at 1035-1045 cm^{-1} as it is obscured by another characteristic vibration of DBT itself.

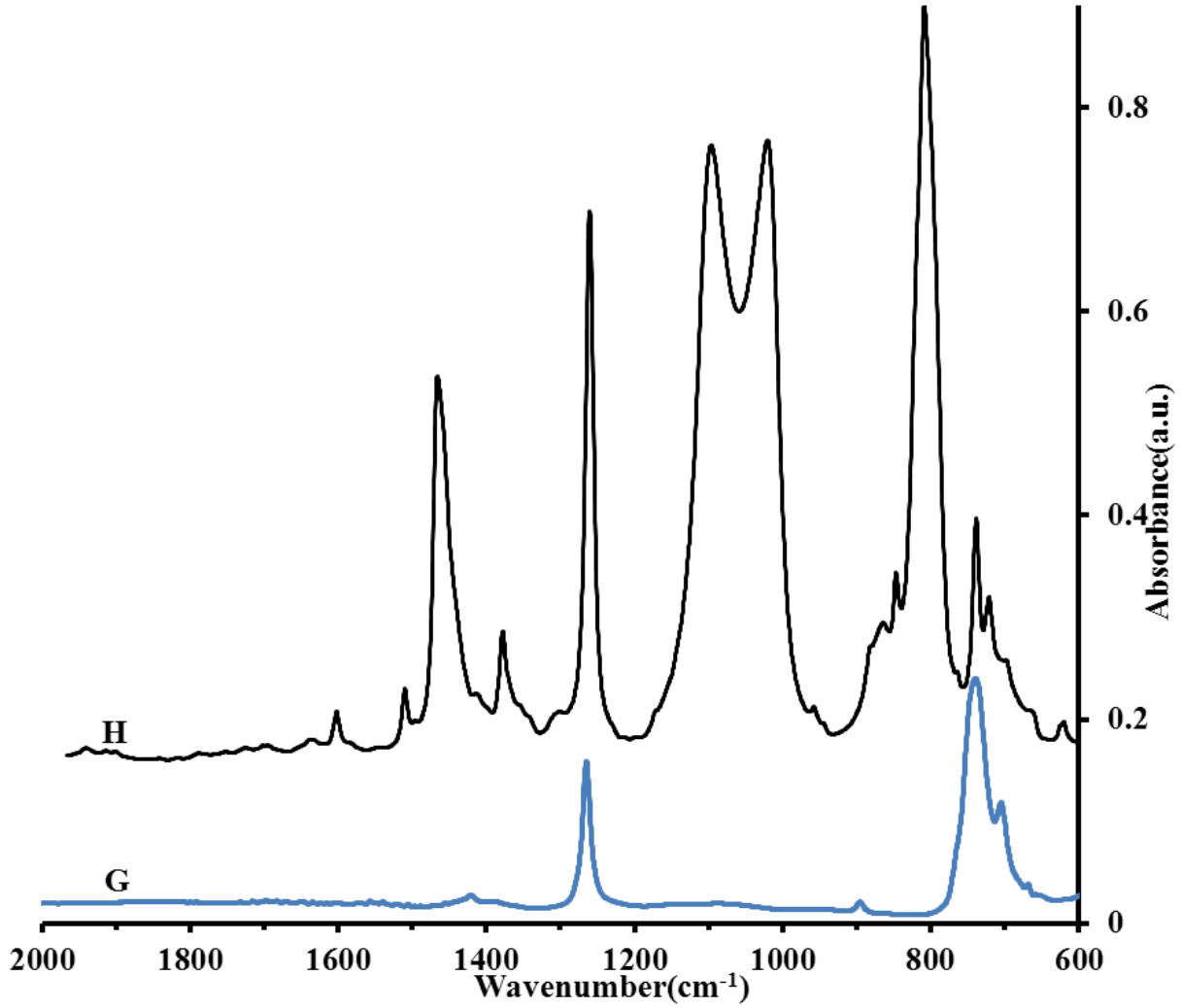

Figure 3.17 FTIR spectra for DCM extractions. G is pure DCM, and H is the AC-02 extract

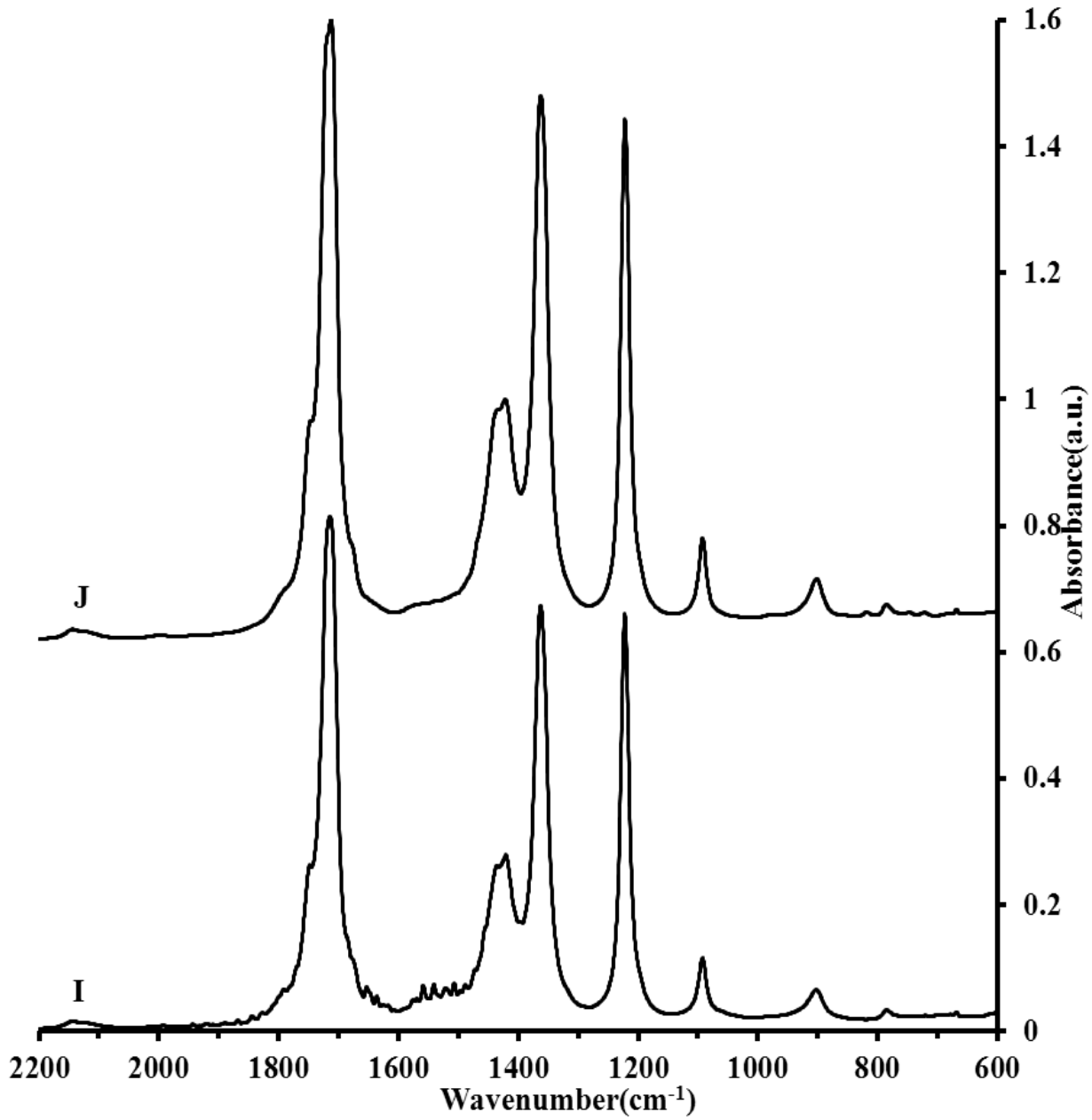

Figure 3.18 FTIR spectra of acetone extract; I is pure solvent, and J is AC-01 extract

The spectrum of an acetone extract is shown in Fig. 3.18; spectrum I is pure acetone, and spectrum J is the extract from AC-01. At 750-830 cm^{-1} there are small peaks that corresponds to the largest peaks for DBT and thiophene. But there is nothing to indicate the presence of sulfones or sulfoxides in this extract.

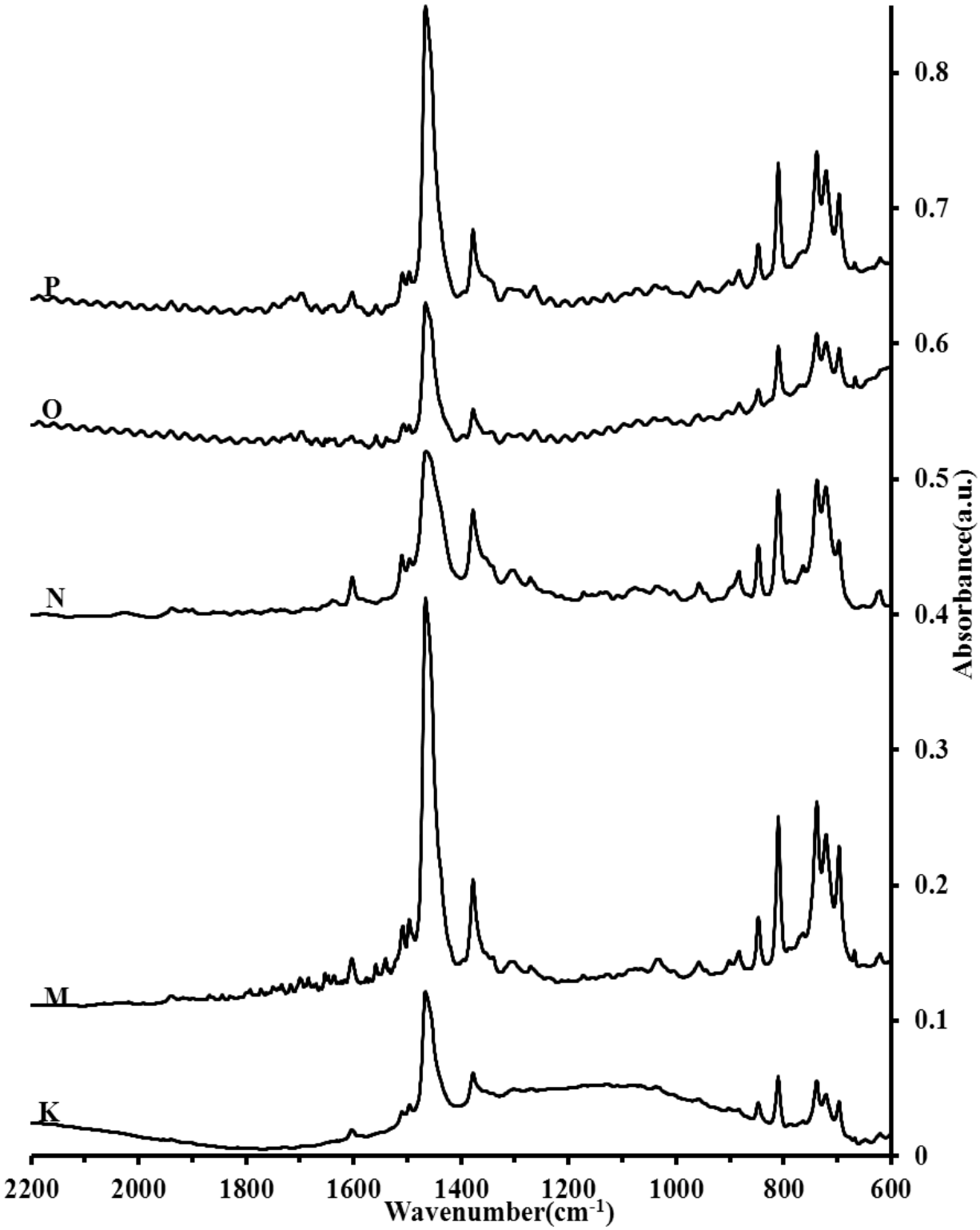

Figure 3.19 FTIR spectra where K is the unreacted feed, M is the AC-01 96 h sample, N is the AC-02 96 h, O is the 383 K AC-03 sample, and P is the 403 K AC-03 sample.

Fig. 3.19 shows FTIR spectra of some feed and product samples removed from the autoclave reactor. Spectrum K is the unreacted light feed sample, spectrum M is the 96 h sample from run AC-01, spectrum N is the 96 h sample from run AC-02,and spectra O and P are the 383 K and 403 K samples, respectively, from run AC-03. The C=O stretch for a carboxylic acid is located at 1710 cm^{-1}, which is visible in M, O, and P. For ketones the stretch is located at approximately 1715 cm^{-1}, and is visible in M. For aldehydes it is located at 1725 cm^{-1}, and is visible in M, O, and P. It appears that spectrum N has (relative to the feed) a bigger water peak, a bigger peak in the sulfone region of 1365-1380 cm^{-1}, as well as a bigger peak in the 650 cm^{-1} sulfone region.

CHAPTER 4 SUMMARY AND CONCLUSIONS

The Ti-MCM-41 catalyst evidenced higher initial activity than the supported Pd/C in the autoclave reactor. But for overall conversion the Pd/E was better. It was noticed that the Ti-MCM-41 catalyst had the greatest observable amount of product on the surface. As a result, it probably deactivated more quickly because of blocked pores and irreversible adsorption on surface sites. The peroxide run with Pd/E catalyst had an initial rate slower than the Ti-MCM-41, but achieved the same overall conversion. Table 4.1 compares all of the overall conversion values for the autoclave runs; it is important to consider how much oxidant was present in the runs. The oxide to feed molar ratio in the reactors was about 20% for the peroxide oxidant and about 25% for the O_2. These ratios were calculated assuming that hexadecane does not react, which agreed with the MS results. The results showed that given roughly the same amounts of oxidant, the amount of oxidation taking place is the same.

Table 4.1: Overall conversion values for autoclave and POMR runs (363 K)

	AC-01	AC-02	AC-03	AC-04	PDM-02	FD401	PDM-6
Catalysts	Eimer	Pd/E	Co Octoate	Pd/E	Pd-monolith	Pd-powder	Pd-Monolith
Oxidant	O_2	O_2	O_2	peroxide	O_2	O_2	peroxide
Time, h	96	96	48	48	6	4	12
Overall Conv.[1]	18%	33%	7.9%	18%	9.4%	11%	20%

[1]Calculated as: 100 x (mols reagent - mols reagent at t=0)/(mols reagent at t=0)

For AC-02, 93% of the moles converted are from ethylbenzene, in agreement with the MS results. The MS found large amounts of ACP, MBM, and DBP. It is possible that DBP is at least partially responsible for an overall conversion higher than the amount of oxidant present, because the stoichiometry for DBP is not 1 to 1 oxygen/ EB, as shown in Fig. 4.1.

The other autoclave runs gave overall conversion values below the amount of oxidant supplied. The Co octoate (Run AC-03 Table 3.7) gave the lowest TOF and lowest overall

conversion; at 98 hours there was still only 15.9% conversion, and this after a temperature increase at 48 hours to 383 K and another at 72 hours to 403 K, as shown in Fig. 4.2. While Co octoate was the least active catalyst, it was the most selective initially. But from Table 3.6 it is seen that the selectivity decreases as the temperature increases outside the normal experimental range.

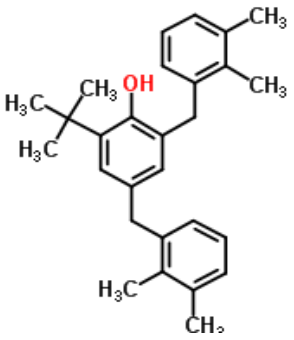

Figure 4.1: (DBP) 2,4-bis(dimethylbenzyl)-6-t-butylphenol

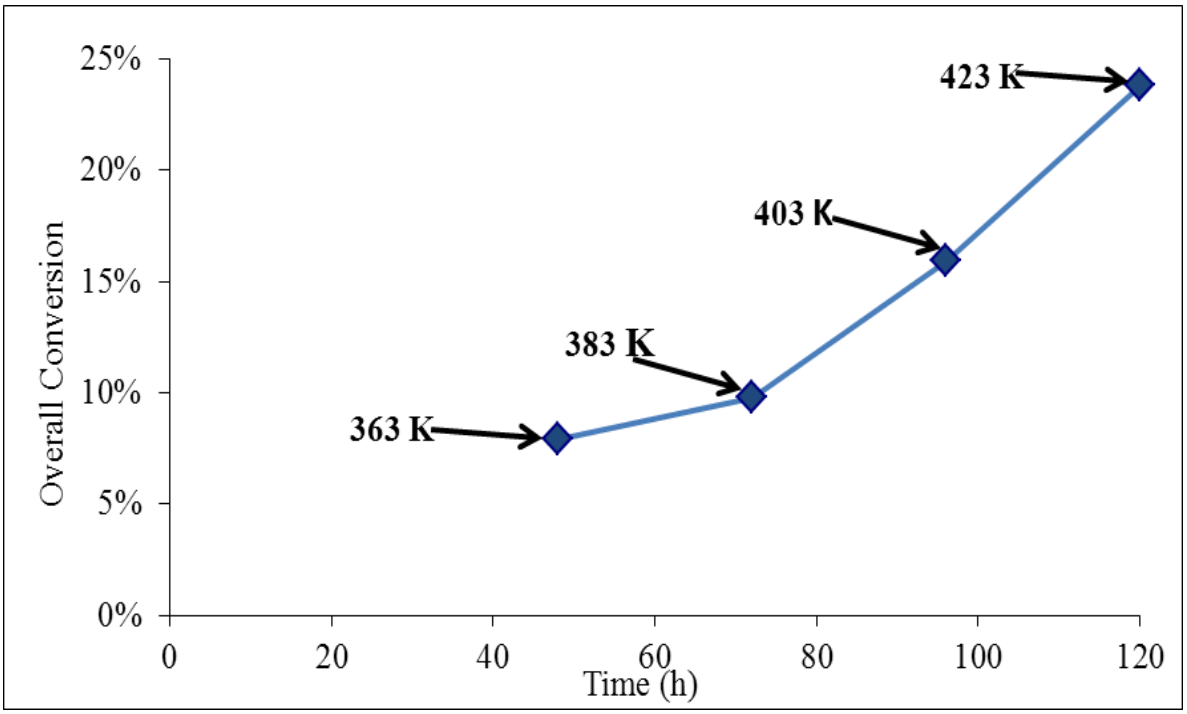

Figure 4.2: AC-03 overall conversion at ramped temperatures

In comparing the oxidation rate of the POMR and autoclave reactor it was shown that the POMR reactor gave a higher initial TOFs than the autoclave, but as it was not possible to run this reactor for 96 h it was impossible to compare overall final conversions. The POMR though had the additional advantage of an unlimited supply of oxidant because the regulator had to be open to keep the pressure equalized over the oscillating diaphragm. The selectivity as shown in Table 4.2 is much higher for the autoclave; every autoclave run had a higher selectivity than the POMR at the same 363 K temperature. The POMR showed the highest TOFs probably because of transport enhancements resulting from the pulsations.

The only POMR run with a substantial DBT conversion was run PDM-2, which was conducted with the "heavy" feed; otherwise thiophene was preferentially oxidized. Considering the results with no catalyst (Tables 3.3 and 3.4), it appeared that oxidation can take place both on the catalyst and in solution. The free radical intermediates existing in solution are generated chiefly from the oxidation reaction of the alkylaromatics, as part of a classical autoxidation mechanism. The higher selectivity associated with certain catalysts likely reflects their better ability to generate peroxidic intermediates, which would interact with the radicals in solution, but might also preferentially oxidize adsorbed sulfur compounds. This would explain the result that as the catalyst deactivated or was inhibited, the selectivity decreased (Table 3.6).

Table 4.2 Selectivity values for final samples at 363 K

Reactor	Autoclave				POMR		
Name	AC-01	AC-02	AC-03	AC-04	PDM-02	FD401	PDM-6
Catalyst Type	"Eimer"	Pd/E	Cobalt Octoate	Pd/E (peroxide)	Monolith Pd	PdP-001 Powder	Monolith Pd (peroxide)
Selectivity	0.095	0.073	0.11	0.033[1]	0.030	0.061	0.078[2]

[1]The thiophene peak was obscured by another product so this selectivity is based on DBT as the only sulfur compound.
[2]Same peroxide to feed ratio as the autoclave, but thiophene conversion could be measured.

Product analyses were conducted, and because the products were difficult to identify by FTIR, FTIR was replaced as the primary technique by GC/MS. Observed reaction products included: acetophenone and α-methylbenzenemethanol from ethylbenzene, 1- and 2-naphthalene carboxaldehyde from methylnaphthalene, DBT sulfones, a pyridinedicarboxylic acid and benzo(h)quinoline from acridine, and indole from carbazole.

The last notable element of this work was the synthesis of an effective monolith coated with Pd-loaded carbon. A Pd loading of up to 5.9% was measured on an activated carbon that was made from a polymer attached to and then carbonized onto a cordierite monolith at 6-12% carbon to monolith ratios. Experiments showed that this catalyst was as effective for ODS as the commercial Pd/C catalyst powders.

REFERENCES

1. Liu, D. Catalytic oxidative desulfurization of a model diesel. Louisiana State University, 2010.

2. Bussard, A. Heterogeneous catalyzed macromolecular hydrogenations in oscillating systems. Louisiana State University, 2008.

3. EPA, U. S., Regulatory Announcement: Heavy-Duty Engine and Vehicle Standards and Highway Fuel Sulfur Control Requirements. December, 2000.

4. Bacha, J., Freel, J., Gibbs, A., Gibbs, L., Hemighaus, G., Hoekman, K., Horn, J., Ingham, M., Jossens, L., Kohler, D., Lesnini, D., McGeehan, J., Nikanjam, M., Olsen, E., Organ, R., Scott, B., Sztenderowicz, M., Tiedemann, A., Walker, C., Lind, J., Jones, J., Scott, D., Mills J. *Chevron Diesel Fuels Technical Review*; Chevron: 2007.

5. (a) Babich, I. V.; Moulijn, J. A., Science and technology of novel processes for deep desulfurization of oil refinery streams: A review. *Fuel* **2003,** *82* (6), 607-631; (b) Attar, A., Corcoran, W. A., Desulfurization of oragnic sulfur compounds by selective oxidation: Regenerable and nonregeneravle oxygen carriers. *Industrial & Engineering Chemistry Project Research and Development* **1978,** *17* (2), 102.

6. Schatterman, Ultrasound assisted oxidative desulfurization. *NPFA Annual Meeting* **2010,** (AM-10-153).

7. Ma, X. L.; Zhou, A. N.; Song, C. S., A novel method for oxidative desulfurization of liquid hydrocarbon fuels based on catalytic oxidation using molecular oxygen coupled with selective adsorption. *Catal Today* **2007,** *123* (1-4), 276-284.

8. Murata, S.; Murata, K.; Kidena, K.; Nomura, M., A novel oxidative desulfurization system for diesel fuels with molecular oxygen in the presence of cobalt catalysts and aldehydes. *Energ Fuel* **2004,** *18* (1), 116-121.

9. Caero, L. C.; Hernandez, E.; Pedraza, F.; Murrieta, F., Oxidative desulfurization of synthetic diesel using supported catalysts - Part I. Study of the operation conditions with a vanadium oxide based catalyst. *Catal Today* **2005,** *107-08*, 564-569.

10. (a) Shiraishi, Y.; Naito, T.; Hirai, T., Vanadosilicate molecular sieve as a catalyst for oxidative desulfurization of light oil. *Ind Eng Chem Res* **2003,** *42* (24), 6034-6039; (b) De Filippis, P.; Scarsella, M., Oxidative desulfurization: Oxidation reactivity of sulfur compounds in different organic matrixes. *Energ Fuel* **2003,** *17* (6), 1452-1455; (c) Rao, T. V.; Sain, B.; Kafola, S.; Sharma, Y. K.; Nanoti, S. M.; Garg, M. O., Oxidative desulfurization of HDS diesel using the aldehyde/molecular oxygen oxidation system. *Energ Fuel* **2007,** *21* (6), 3420-3424; (d) Lu, Y.; Wang, Y.; Gao, L. D.; Chen, J. C.; Mao, J. P.; Xue, Q. S.; Liu, Y.; Wu, H. H.; Gao, G. H.; He, M. Y., Aerobic oxidative desulfurization: A promising approach for sulfur removal from fuels. *Chemsuschem* **2008,** *1* (4), 302-306; (e) Otsuki, S.; Nonaka, T.; Takashima, N.; Qian, W. H.;

Ishihara, A.; Imai, T.; Kabe, T., Oxidative desulfurization of light gas oil and vacuum gas oil by oxidation and solvent extraction. *Energ Fuel* **2000,** *14* (6), 1232-1239.

11. Sampanthar, J. T.; Xiao, H.; Dou, H.; Nah, T. Y.; Rong, X.; Kwan, W. P., A novel oxidative desulfurization process to remove refractory sulfur compounds from diesel fuel. *Appl Catal B-Environ* **2006,** *63* (1-2), 85-93.

12. (a) Fang, Y. M.; Hu, H. Q., Mesoporous TS-1: Nanocasting synthesis with CMK-3 as template and its performance in catalytic oxidation of aromatic thiophene. *Catal Commun* **2007,** *8* (5), 817-820; (b) Batiagalhia, F. e. a., Selective and mild oxidation of sulfides to sulfoxides by oxodiperoxo molybdenum complexes adsorbed onto silica gel. *Tetrahedron* **2001,** *39*, 9669-9676; (c) Hulea, V.; Fajula, F.; Bousquet, J., Mild oxidation with H2O2 over Ti-containing molecular sieves - A very efficient method for removing aromatic sulfur compounds from fuels. *J Catal* **2001,** *198* (2), 179-186; (d) Hulea, V.; Moreau, P.; DiRenzo, F., Thioether oxidation by hydrogen peroxide using titanium-containing zeolites as catalysts. *J Mol Catal a-Chem* **1996,** *111* (3), 325-332; (e) Vetter, A., Berkessel, A., Schiff-base ligands carrying two elements of chirality: Matched-mismatched effects in the vanadium-catalyzed sulfoxidation of thioethers with hydrogen peroxide. *Tetrahedron Lettters* **1998,** *39*, 1741-1744.

13. Kaczorowska, K.; Kolarska, Z.; Mitka, K.; Kowalski, P., Oxidation of sulfides to sulfoxides. Part 2: Oxidation by hydrogen peroxide. *Tetrahedron* **2005,** *61* (35), 8315-8327.

14. Zhao, D.; Ren, H.; Wang, J.; Yang, Y.; Zhao, Y., Kinetics and mechanism of quaternary ammonium salts as phase-transfer catalysts in the liquid-liquid phase for oxidation of thiophene. *Energ Fuel* **2007,** *21* (5), 2543-2547.

15. Li, C.; Jiang, Z. X.; Gao, J. B.; Yang, Y. X.; Wang, S. J.; Tian, F. P.; Sun, F. X.; Sun, X. P.; Ying, P. L.; Han, C. R., Ultra-deep desulfurization of diesel: Oxidation with a recoverable catalyst assembled in emulsion. *Chem-Eur J* **2004,** *10* (9), 2277-2280.

16. Chica, A.; Corma, A.; Domine, M. E., Catalytic oxidative desulfurization (ODS) of diesel fuel on a continuous fixed-bed reactor. *J Catal* **2006,** *242* (2), 299-308.

17. de Angelis, A.; Pollesel, P.; Molinari, D.; Parker, W. O.; Frattini, A.; Cavani, F.; Martins, S.; Perego, C., Heteropolyacids as effective catalysts to obtain zero sulfur diesel. *Pure Appl Chem* **2007,** *79* (11), 1887-1894.

18. Mei, H.; Mei, B. W.; Yen, T. F., A new method for obtaining ultra-low sulfur diesel fuel via ultrasound assisted oxidative desulfurization. *Fuel* **2003,** *82* (4), 405-414.

19. Mikkola, J. P.; Salmi, T., Three-phase catalytic hydrogenation of xylose to xylitol prolonging the catalyst activity by means of on-line ultrasonic treatment. *Catal Today* **2001,** *64* (3-4), 271-277.

20. (a) Flint, E. B.; Suslick, K. S., The Temperature of Cavitation. *Science* **1991,** *253* (5026), 1397-1399; (b) Prozorov, T.; Prozorov, R.; Suslick, K. S., High velocity interparticle collisions driven by ultrasound. *J Am Chem Soc* **2004,** *126* (43), 13890-13891.

21. Flannigan, D. J.; Hopkins, S. D.; Camara, C. G.; Putterman, S. J.; Suslick, K. S., Measurement of pressure and density inside a single sonoluminescing bubble. *Phys Rev Lett* **2006,** *96* (20).

22. Doktycz, S. J.; Suslick, K. S., Interparticle Collisions Driven by Ultrasound. *Science* **1990,** *247* (4946), 1067-1069.

23. Suslick, K. S.; Mdleleni, M. M.; Ries, J. T., Chemistry induced by hydrodynamic cavitation. *J Am Chem Soc* **1997,** *119* (39), 9303-9304.

24. Suslick, K. S.; Casadonte, D. J., Heterogeneous Sonocatalysis with Nickel Powder. *J Am Chem Soc* **1987,** *109* (11), 3459-3461.

25. (a) Gunnerman, R. Upgrading of petroleum by combined ultrasound and microwave treatments. US 20060180500A1, 2006; (b) Gunnerman, R. Continuous process for oxidatidative desulfurization of fossil fuels with ultrasound and products thereof. US6500219, 2002; (c) al, Y. e. Oxidative desulfurization of fossil fuels with ultrasound. US 6402939 B1, 2002; (d) al, G. e. Loop-shaped ultrasound generator and use in reaction systems. US 2006/0260405 A1, 2006.

26. Roy, S.; Bauer, T.; Al-Dahhan, M.; Lehner, P.; Turek, T., Monoliths as multiphase reactors: A review. *Aiche Journal* **2004,** *50* (11), 2918-2938.

27. Herskowitz, M.; Smith, J. M., Trickle-Bed Reactors - a Review. *Aiche Journal* **1983,** *29* (1), 1-18.

28. (a) Lange, R.; Hanika, J.; Stradiotto, D.; Hudgins, R. R.; Silveston, P. L., Investigations of periodically operated trickle-bed reactors. *Chem Eng Sci* **1994,** *49* (24B), 5615-5621; (b) Boelhouwer, J. G.; Piepers, H. W.; Drinkenburg, A. A. H., Nature and characteristics of pulsing flow in trickle-bed reactors. *Chem Eng Sci* **2002,** *57* (22-23), 4865-4876; (c) Boelhouwer, J. G.; Piepers, H. W.; Drinkenburg, A. A. H., Liquid-induced pulsing flow in trickle-bed reactors. *Chem Eng Sci* **2002,** *57* (16), 3387-3399; (d) Blok, J. R.; Drinkenburg, A. A. H., Hydrodynamic Properties of Pulses in 2-Phase Downflow Operated Packed-Columns. *Chem Eng J Bioch Eng* **1982,** *25* (1), 89-99; (e) Castellari, A., Haure, P., Experimental-Study of the Periodic Operatio of a Trickle Bed Reactor. *Aiche Journal* **1995,** *41* (6), 1593-1597; (f) Khadilkar, M. R.; Al-Dahhan, M. H.; Dudukovic, M. P., Parametric study of unsteady-state flow modulation in trickle-bed reactors. *Chem Eng Sci* **1999,** *54* (13-14), 2585-2595.

29. Wilhite, B. A.; Huang, X.; McCready, M. J.; Varma, A., Effects of induced pulsing flow on trickle-bed reactor performance. *Ind Eng Chem Res* **2003,** *42* (10), 2139-2145.

30. Harvey, A. P.; Mackley, M. R.; Seliger, T., Process intensification of biodiesel production using a continuous oscillatory flow reactor. *J Chem Technol Biot* **2003,** *78* (2-3), 338-341.

31. (a) Gao, S.; Ni, X.; Cumming, R. H.; Greated, C. A.; Norman, P., Experimental investigation of bentonite flocculation in a batch oscillatory baffled column. *Separ Sci Technol* **1998,** *33* (14), 2143-2157; (b) Wilson, B.; Ni, X.; Sherrington, D. C., On the investigation of a phase-transfer catalysis reaction in an oscillatory baffled reactor. *Ind Eng Chem Res* **2001,** *40* (23), 5300-5304; (c) Ni, X.; Bennett, D. C.; Symes, K. C.; Grey, B. D., Inverse phase suspension polymerization of acrylamide in a batch oscillatory raffled reactor. *J Appl Polym Sci* **2000,** *76* (11), 1669-1676.

32. Fabiyi, M. E.; Skelton, R. L., Photocatalytic mineralisation of methylene blue using buoyant TiO2-coated polystyrene beads. *J Photoch Photobio A* **2000,** *132* (1-2), 121-128.

33. Windom, B. C.; Huber, M. L.; Bruno, T. J.; Lown, A. L.; Lira, C. T., Measurements and Modeling Study on a High-Aromatic Diesel Fuel. *Energ Fuel* **2012,** *26* (3), 1787-1797.

34. Ramos, A. L. D.; Alves, P. D.; Aranda, D. A. G.; Schmal, M., Characterization of carbon supported palladium catalysts: inference of electronic and particle size effects using reaction probes. *Applied Catalysis a-General* **2004,** *277* (1-2), 71-81.

35. Toebes, M. L.; van Dillen, J. A.; de Jong, Y. P., Synthesis of supported palladium catalysts. *J Mol Catal a-Chem* **2001,** *173* (1-2), 75-98.

36. Eimer, G. A.; Casuscelli, S. G.; Ghione, G. E.; Crivello, M. E.; Herrero, E. R., Synthesis, characterization and selective oxidation properties of Ti-containing mesoporous catalysts. *Applied Catalysis a-General* **2006,** *298*, 232-242.

37. (a) Wang, X. Q.; Liang, C. D.; Dai, S., Facile synthesis of ordered mesoporous carbons with high thermal stability by self-assembly of resorcinol-formaldehyde and block copolymers under highly acidic conditions. *Langmuir* **2008,** *24* (14), 7500-7505; (b) Bazula, P. A.; Lu, A. H.; Nitz, J. J.; Schuth, F., Surface and pore structure modification of ordered mesoporous carbons via a chemical oxidation approach. *Micropor Mesopor Mat* **2008,** *108* (1-3), 266-275.

38. (a) Stein(director), S. E., "Infrared Specra. NIST Mass Spec Data Center: 2012; (b) Keller, R. J., *Sigma Library of FTIR Spectra, Volumes 1 and 2*. Sigma Chemical Company: Sigma Chemical Company, 1986.

APPENDIX: GC CALIBRATION

To calibrate the GC a series of calibration samples were made by adding the fixed amount of internal standard (mesitylene) to the feed solution in which the composition are already known. And then each sample was analyzed by HP 5890 GC three times. The $f_i$calibration factor of compound i can be computed through Eq. A.1

$$f_i = \frac{A_i/A_s}{C_i/C_s} \quad \text{Eq.A.1}$$

In Eq.A.1, A_i is the peak area of compound i while A_s is the peak area of internal standard s. C_i is the molar concentration of compound I and C_s is the molar concentration of internal standard s.

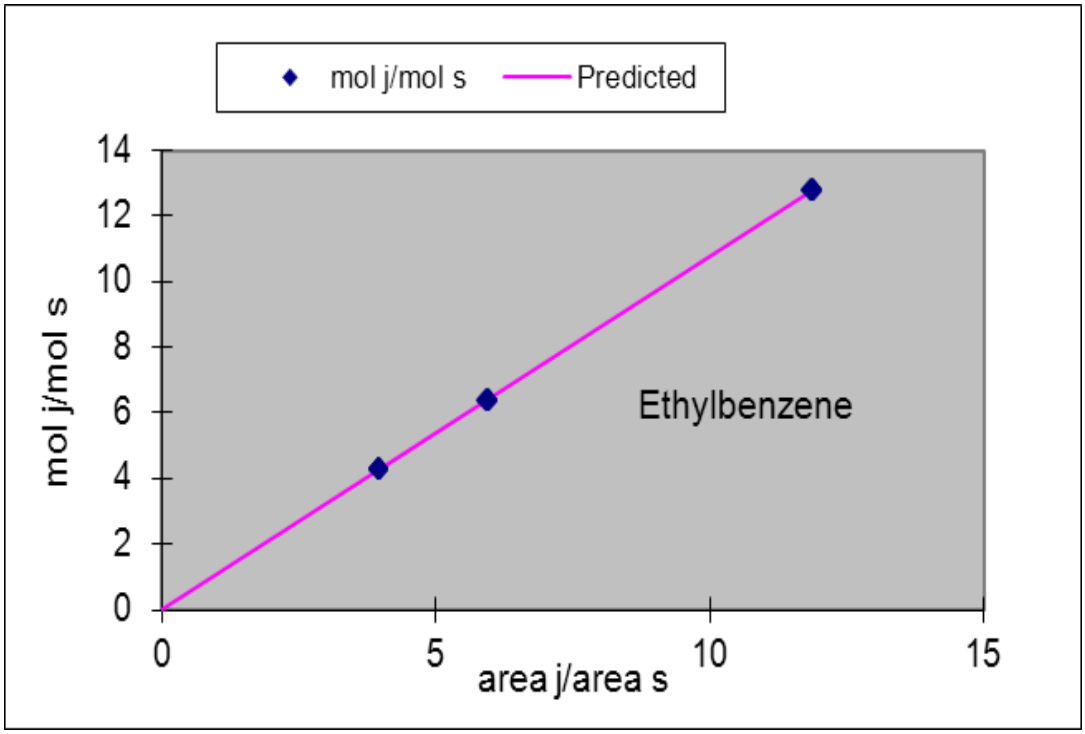

Figure A.1 Calibration curve for ethylbenzene

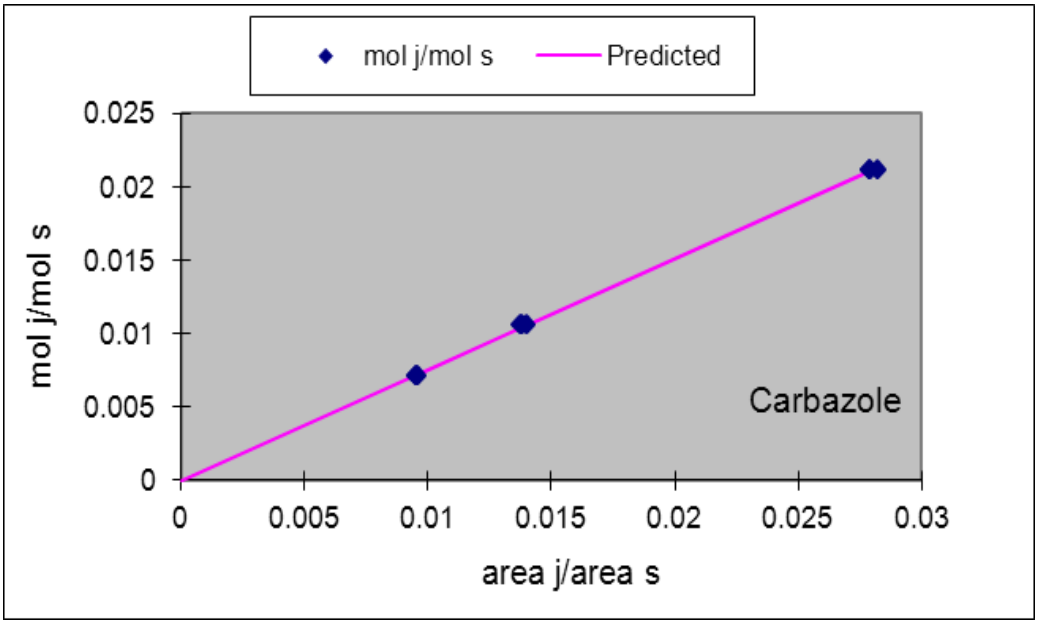

Figure A.2 Calibration curve for carbazole

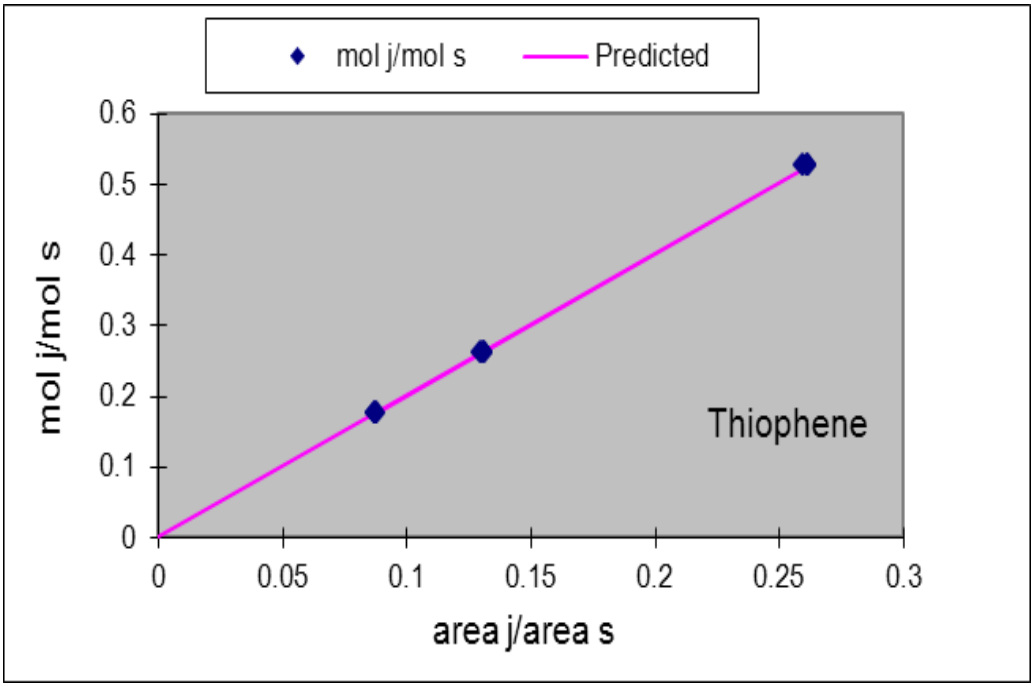

Figure A.3 Calibration Curve for thiophene

VITA

Andrew Madrid was born to Larry and Connie Madrid in Lakeland, FL. His father, a civil engineer, inspired his career choice and starting in 2004, Andrew enrolled at the University of Florida in Gainesville, FL, majoring in chemical engineering. This degree was obtained in 2010; he then attended Louisiana State University earning his MSChE, and now is moving to Charleston, SC to be with his wife, Chelsea. He looks forward to a career in industry and to eventually getting his PhD in chemical engineering.